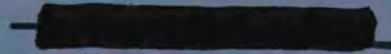


OAK RIDGE NATIONAL LABORATORY LIBRARIES



3 4456 0549168 8



CENTRAL RESEARCH LIBRARY
DOCUMENT COLLECTION

OAK RIDGE NATIONAL LABORATORY

operated by

UNION CARBIDE CORPORATION

for the

U.S. ATOMIC ENERGY COMMISSION



ORNL - TM - 960

/

FUELS AND MATERIALS DEVELOPMENT PROGRAM QUARTERLY PROGRESS REPORT

FOR PERIOD ENDING SEPTEMBER 30, 1964

DECLASSIFIED

CLASSIFICATION CHANGED TO:

BY AUTHORITY OF AECM-2104 a2 B6 8/21/74
BY BL Rudd

**CENTRAL RESEARCH LIBRARY
DOCUMENT COLLECTION
LIBRARY LOAN COPY
DO NOT TRANSFER TO ANOTHER PERSON**
If you wish someone else to see this document, send in name with document and the library will arrange a loan.

NOTICE

This document contains information of a preliminary nature and was prepared primarily for internal use at the Oak Ridge National Laboratory. It is subject to revision or correction and therefore does not represent a final report. The information is not to be abstracted, reprinted or otherwise given public dissemination without the approval of the ORNL patent branch, Legal and Information Control Department.



LEGAL NOTICE

This report was prepared as an account of Government sponsored work. Neither the United States, nor the Commission, nor any person acting on behalf of the Commission:

- A. Makes any warranty or representation, expressed or implied, with respect to the accuracy, completeness, or usefulness of the information contained in this report, or that the use of any information, apparatus, method, or process disclosed in this report may not infringe privately owned rights; or
- B. Assumes any liabilities with respect to the use of, or for damages resulting from the use of any information, apparatus, method, or process disclosed in this report.

As used in the above, "person acting on behalf of the Commission" includes any employee or contractor of the Commission, or employee of such contractor, to the extent that such employee or contractor of the Commission, or employee of such contractor prepares, disseminates, or provides access to, any information pursuant to his employment or contract with the Commission, or his employment with such contractor.

Contract No. W-7405-eng-26

FUELS AND MATERIALS DEVELOPMENT PROGRAM QUARTERLY PROGRESS REPORT
FOR PERIOD ENDING SEPTEMBER 30, 1964

Compiled by

P. Patriarca

NOVEMBER 1964

OAK RIDGE NATIONAL LABORATORY
Oak Ridge, Tennessee
operated by
UNION CARBIDE CORPORATION
for the
U.S. ATOMIC ENERGY COMMISSION



OAK RIDGE NATIONAL LABORATORY LIBRARIES

3 4456 0549168 8

FOREWORD

This is the second quarterly progress report describing work performed at the Oak Ridge National Laboratory for the Fuels and Materials Development Branch, Division of Reactor Development, U. S. Atomic Energy Commission. The specific programs covered are as follows:

<u>Program Title</u>	<u>Person in Charge</u>	<u>Principal Investigator(s)</u>
Fuel Element Development	G. M. Adamson, Jr.	C. F. Leitten, Jr. J. P. Hammond
Nondestructive Test Development	D. A. Douglas, Jr.	R. W. McClung
Solid Reaction Studies	C. J. McHargue	T. S. Lundy
Zirconium Metallurgy	C. J. McHargue	M. L. Picklesimer

TABLE OF CONTENTS

	Page
Summary	v
1. Fuel Element Development	1
Deposition of Refractory Uranium Compounds	1
Deposition of Tungsten Alloys	2
Fabrication of Aluminum-Base Irradiation Test Plates	6
Hydrogen Absorption in the Water-Vapor Aluminum System	9
Fabrication of Uranium Monocarbide with Fugitive Sintering Aids	10
2. Nondestructive Test Development	15
Electromagnetic Test Development	15
Ultrasonic Test Methods	17
Penetrating Radiation	20
Gamma Scintillation Gaging	20
X-Ray Imaging with Closed-Circuit Television	21
Inspection Development of Problem Materials	21
3. Solid Reaction Studies	22
Diffusion of Nb ⁹⁵ Into Tantalum Single Crystals	22
Introduction	22
Experimental Procedure	23
Results and Discussion	24
Conclusions	33
Acknowledgments	34
References	34
4. Zirconium Metallurgy	36
Zirconium Alloys	36
Anisotropy in Zircaloy-2	37
The Effect of Preferred Orientation and Stress on the Directional Precipitation of Hydrides in Zircaloy-2	38
Optical Properties of Zirconium Alloys	41



Preparation of Single Crystals of Zirconium and Zirconium Alloys	44
Zone Refining of Zirconium	45
Properties of High-Purity Zirconium	46
Oxide Film Studies	46



SUMMARY

1. Fuel Element Development

We can obtain a dense solid deposit of UO_2 using thermochemical deposition techniques by lowering the system pressure and increasing the ratio of fuel gas to hydrogen. Metallography revealed a large-grained two-phase deposit. Control over the system has been increased by substituting oxygen for water vapor as the oxidizing gas.

We are encountering difficulty in reproducibly depositing tungsten-rhenium tubing; however, we have proved the feasibility of the technique. A tube 5 in. long containing 33% Re with a variation in composition of 3.5% was deposited. Computer programs have been established to reduce the number of test runs required.

Homogeneity examinations were completed on the miniature aluminum-base fuel plates that had been fabricated previously. The plates containing U_3O_8 dispersions were satisfactory; however, those with coated UO_2 particles showed excessive variation in uranium content and poor distribution. Plates of the latter type were made using individually pressed cores rather than ones machined from large compacts; excellent dimensional and uranium loading and adequate homogeneity control were achieved. We developed a procedure for fabricating instrumented plates containing two cores in which both cores elongated uniformly. In previous processes, one core elongated much more than the other.

Experiments to study hydrogen absorption in aluminum have been clouded by difficulty in obtaining material with a uniform or controlled water content on the surface. We found that the surface picked up water very rapidly, even when the samples were exposed only to air at room temperature.

While UBe_{13} has previously been shown to be an effective sintering aid for uranium carbide, we have found that its effectiveness is seriously impaired by the presence in the carbide of excessive oxygen or above-stoichiometric carbon. Preliminary work indicates such limitations may not apply when U_3Si_2 is used as the sintering aid.

2. Nondestructive Test Development

We are developing new techniques and equipment for the nondestructive evaluation of materials and components. The major emphasis has been on eddy-current, ultrasonic, and penetrating-radiation methods.

Improvements have been made to our analytical approach for the computer calculation of coil impedance and other electromagnetic field parameters. These will eliminate some shortcomings on problems containing permeability variations. Improvements to the phase sensitive eddy-current instrument include higher frequency operation for application to thin, low-resistivity materials and development of time differentiating circuits to enhance flaw detection. Experiments have shown the system to be excellent for cladding-thickness measurements.

We have continued to study techniques for the detection of nonbond in cladding structure with emphasis on aluminum-clad dispersion-core fuel plates. A newly designed two-crystal angle manipulator has been demonstrated to be useful for precision work on Lamb-wave and other two-crystal techniques. We have started studies on fabrication of very shallow reference notches for tubing inspection.

The use of x-ray attenuation scintillation gaging for the determination of total fuel content is being investigated. Measurement of single-point sensitivity for thickness change and radiation-intensity variation has been shown to be about 0.2%. We have started an experiment on the application of an x-ray sensitive closed-circuit television system for measuring fuel expansion during thermal excursion.

In our work on problem materials we have successfully evaluated D-43, T-111, and B-66 alloy tubing, although some difficulty has been encountered on the application of eddy currents.

3. Solid Reaction Studies

We obtained penetration curves for the diffusion of ^{95}Nb into tantalum single crystals at temperatures from 1050 to 1600°C. For the conditions of these experiments, the curves were characterized by a region of large slope near the surface, followed by a region of much lesser slope deeper into the metal. Originally, we thought that the near-surface behavior in this case was anomalous in origin, occurring

as a result of phenomena associated with the extremely small penetration distances. However, the present results indicate that this is probably not the case, the first region being a result of lattice diffusion, while the second portion is a consequence of the presence of short-circuit diffusion paths.

4. Zirconium Metallurgy

We determined the electrical resistivity as a function of alloy content, temperature, and heating and cooling rates for most of a series of zirconium-titanium alloys containing 0, 25, 40, 50, 60, 75, and 100 at. % Ti. The data for the Zr-25 at. % Ti appear to be anomalously high and will be redetermined. We detected no ordering or aging reaction by electrical resistivity in the Zr-50 at. % Ti alloy. The data were obtained preliminary to a study of the specific heats of the same materials at the University of Tennessee. Temperature gradient specimens were also prepared for metallographic examination, but the collection of data is not sufficiently complete for an analysis.

We are constructing a tube-testing device for measuring the anisotropic strain of Zircaloy-2 in biaxial stress as a function of fabrication variables and preferred orientation. The frame has been assembled, most of the parts for the test heads have been machined, and all required instrumentation is on hand.

The redistribution of hydrides precipitated under stress during cooling of Zircaloy-2 is being studied. The data recently obtained confirm our prior conclusion that there is an appreciable redistribution only if the elastic stress is parallel to a concentration of basal poles in the texture considerably greater than random. We also tested specimens at nominal hydrogen contents of 50, 150, and 250 ppm. The number of hydrides at any angle in the control (unstressed) specimens is a function only of hydrogen content, the percent of the total at each angle being identical at all three levels. The higher the hydrogen content, the greater is the number of hydrides reoriented but the fraction reoriented is less. We found the average hydride particle size to be independent of the hydrogen level for this series of specimens. The redistribution of hydrides increased as the stress increased. The

data must be analyzed in terms of the number of hydrides per square centimeter per angular increment rather than in terms of the percent hydrides per angular increment. If this is not done, the data obtained can be misleading.

We are measuring optical properties of single crystals of alpha zirconium for studies of oxide films in situ to permit an unique determination of the crystallographic orientation of an individual grain from a single surface examination and to provide information for the determination of preferred orientation by polarized light microscopy. These techniques will be used to study the variation of the texture from surface-to-center of the wall of tubing, preferential precipitation hydrides in certain grain boundaries, effects of restraint on deformation systems operating in single and multicrystal specimens, etc. Little of the presently available theory appears to be pertinent or usable as a guide for the measurements. Our first measurements are reported for the ellipticity and angle of rotation of polarized light as functions of wavelength and crystal section. The data indicate that successful techniques can be developed for satisfying the objectives.

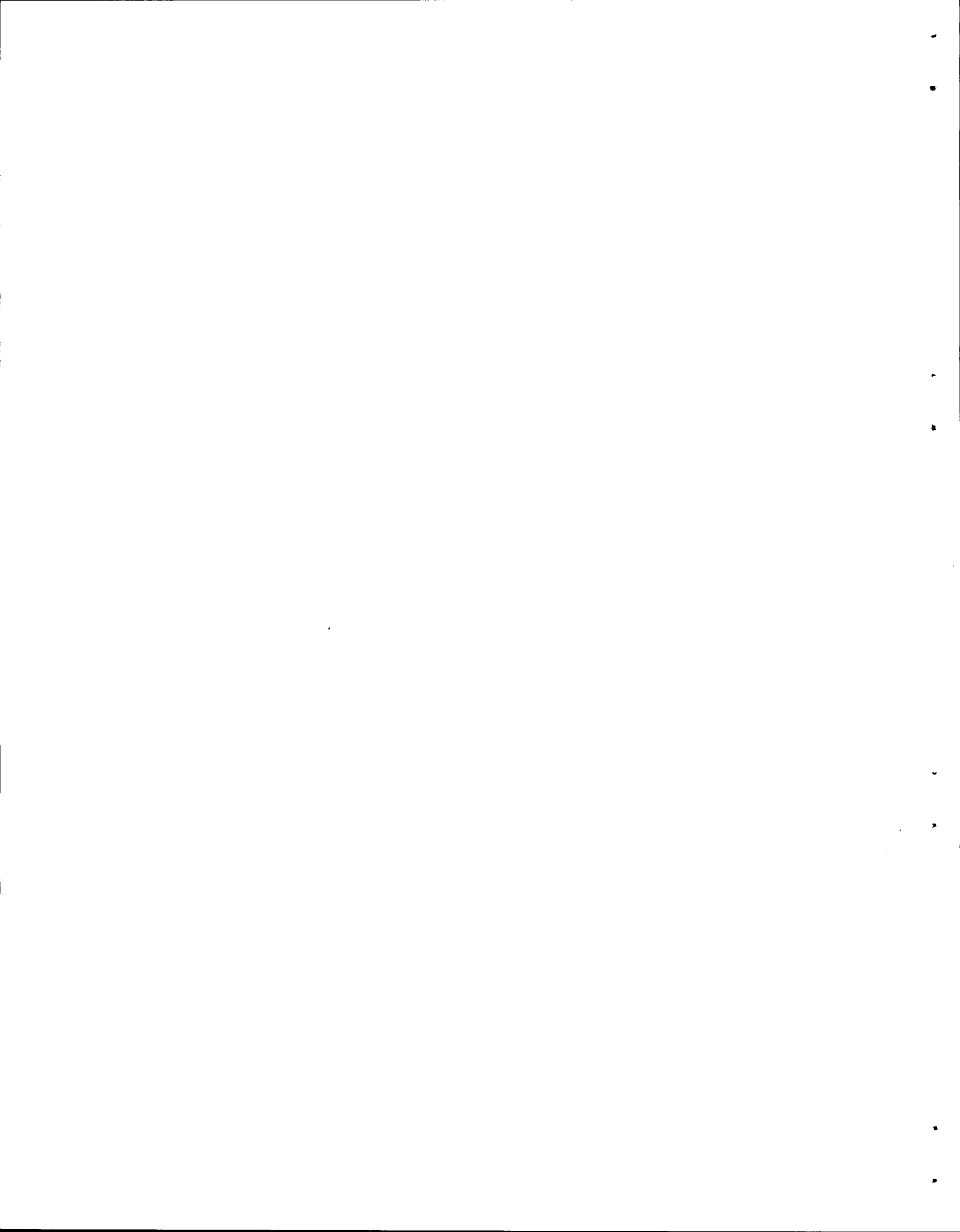
The yield of single crystals of α -zirconium has recently been increased to about 60% by zone melting after seeding. A radiation shield has been used to tilt the trailing α - β interface, causing smaller grains to grow out of the specimen in a shorter traverse distance and subsequently increasing the yield of single crystals.

An electrical discharge machine was constructed for cutting sections of single crystals and shaping single-crystal spheres of α -zirconium. The machining is fast and the surfaces produced are sufficiently good for the specimens to be finished by chemical polishing.

We successfully zone melted an as-deposited bar of iodide zirconium, 3/4 in. across the flats, in the zone-melting equipment originally designed for 1/4-in.-diam rods.

Zone-refined bars of iodide zirconium were cold rolled to strip for studying the effects of impurities on recrystallization and oxidation-corrosion behavior. Specimens cut from the "head" end of the bar completely recrystallized in less than 2 hr at 250°C. We have not learned the purities of the separate sections.

Comparison of the indices of refraction for anodized oxide films in situ and stripped from the zirconium specimens shows that there is appreciable strain present in the film in situ which is relieved when the oxide film is stripped from the specimen.



1. FUEL ELEMENT DEVELOPMENT

G. M. Adamson, Jr.

The objective of the Fuel Element Development Program remains the development of new or improved fabrication techniques for both complete fuel elements and for fuel or cladding materials. We are studying a variety of materials for both uses, selected to include the more promising ones for use at temperatures over a wide range.

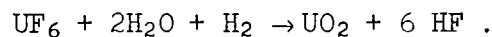
We are presently emphasizing vapor deposition as a fabrication technique. Our ultimate goal is the fabrication of a fuel element by a one-step fuel-conversion process followed by formation of an integral clad, both using the vapor-deposition method. To achieve this goal, separate fabrication efforts have been directed toward the preparation of UO₂ as the fuel material and tungsten and its alloys as the cladding materials.

Improvements in aluminum-base dispersion fuel elements are being sought through a better understanding of their limitations by studies of the operational limits imposed by radiation damage and the mechanism of hydrogen adsorption during fabrication.

Deposition of Refractory Uranium Compounds

R. L. Heestand C. F. Leitten, Jr.

We have continued experiments to determine the feasibility of thermochemical deposition as a one-step technique for fabricating ceramic fuels. As reported previously,¹ we have demonstrated that UO₂ can be produced as a powder, a needle-like crystalline deposit, or a solid using the reaction:



In the previous experiments, however, high-density solid deposits were not obtained. Recent experiments show that a uniform, dense deposit is obtained by increasing the fuel concentration in relation to the hydrogen and water concentration.

¹R. L. Heestand and C. F. Leitten, Jr., Fuels and Materials Development Program Quart. Progr. Rept. June 30, 1964, ORNL-TM-920, pp. 3-7.

Typical conditions for forming a crystalline needle-like deposit are shown in example 1 of Table 1.1. The needles consist of dendritic platelets as shown in Fig. 1.1, which constitute a low-bulk-density material. On raising the UF_6 concentration and lowering system pressure, a more dense deposit was formed at the tops of the needles; and when experiments were run using compositions as shown in example 2, a high-density uniform deposit approximately 6 in. long is obtained. The deposition rate for this type of deposit is comparable to that obtained when depositing metallic tungsten from tungsten hexafluoride.

Wet chemical analysis of the material gives an oxygen-to-uranium ratio of 2.048, and the density found by alcohol immersion is 11.04 g/cm³. Figure 1.2 shows the cross section of a deposit approximately 0.045 in. thick, which was obtained in 4 hr. The second-phase material has not been identified, but corollary fuel work indicates U_4O_9 as a possibility for the observed oxygen-to-uranium ratio.

We also found that oxygen may be substituted for water vapor, as in example 3, to give a comparable high-density deposit; and we anticipate that the use of oxygen will give better composition control, as steam is sometimes difficult to meter.

In the next period, studies of effects of gas composition on the deposit will continue.

Deposition of Tungsten Alloys

J. I. Federer C. F. Leitten, Jr.

Tungsten-rhenium alloy deposition reported previously² showed that gross inhomogeneity of composition and nonuniformity of thickness occurred in tubular deposits prepared at 700°C; a higher rhenium content and greater thickness occurred near the inlet to the reaction zone; and tubular deposits of pure rhenium consisted of thick nodular growths near the inlet to the reaction zone at temperatures above 500°C, but these deposits were

²J. I. Federer and C. F. Leitten, Jr., Fuels and Materials Development Program Quart. Progr. Rept. June 30, 1964, ORNL-TM-920, pp. 7-10.

Table 1.1. Experimental Parameters for Deposition of UO_2

Example	Gas Composition (%)				Temperature (°C)	Pressure (torr)	Products
	H_2	H_2O	O_2	UF_6			
1	78.2	21.5		0.3	1300	6	UO_2
2	79.1	17.3		3.6	1300	3.2	UO_2
3	84.0		12.2	3.8	1300	3.0	UO_2

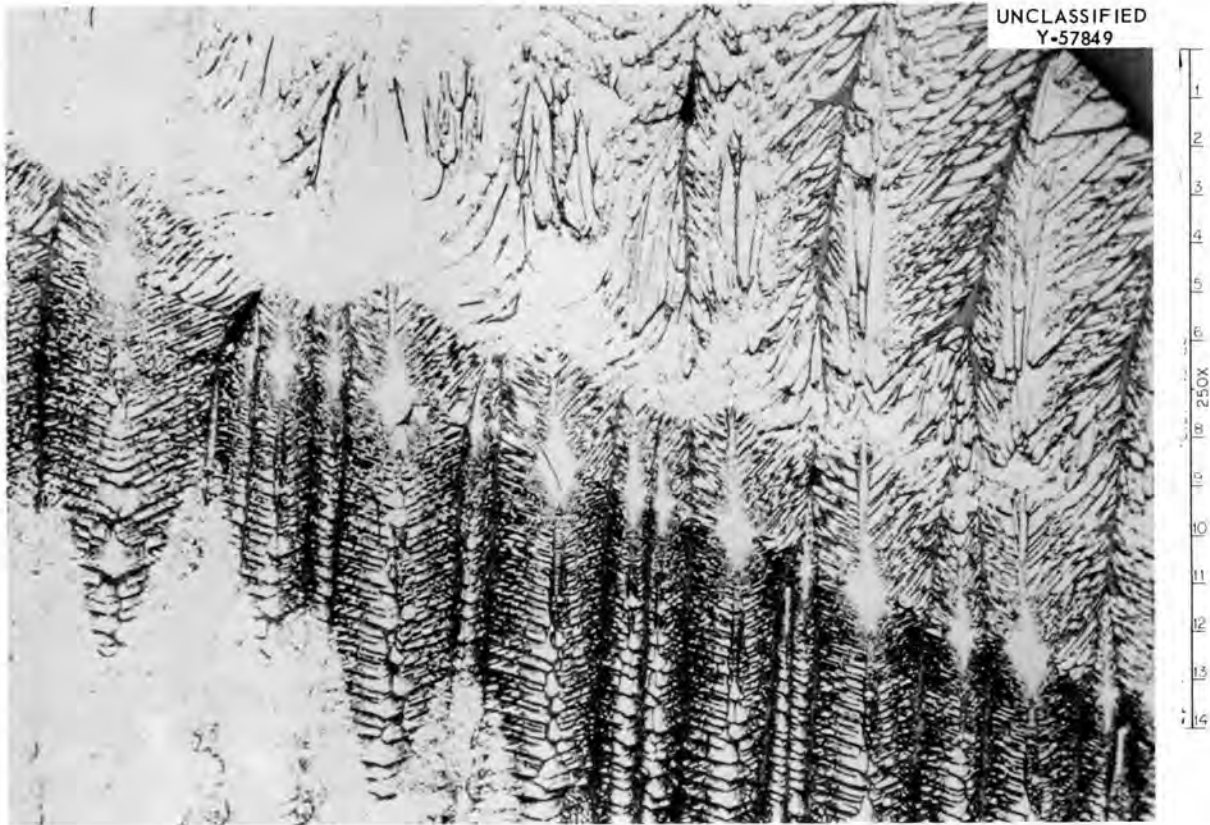


Fig. 1.1. UO_2 Needle Deposit. Etched: 70 H_2O , 20 H_2O_2 (30%), 10 HNO_3 .

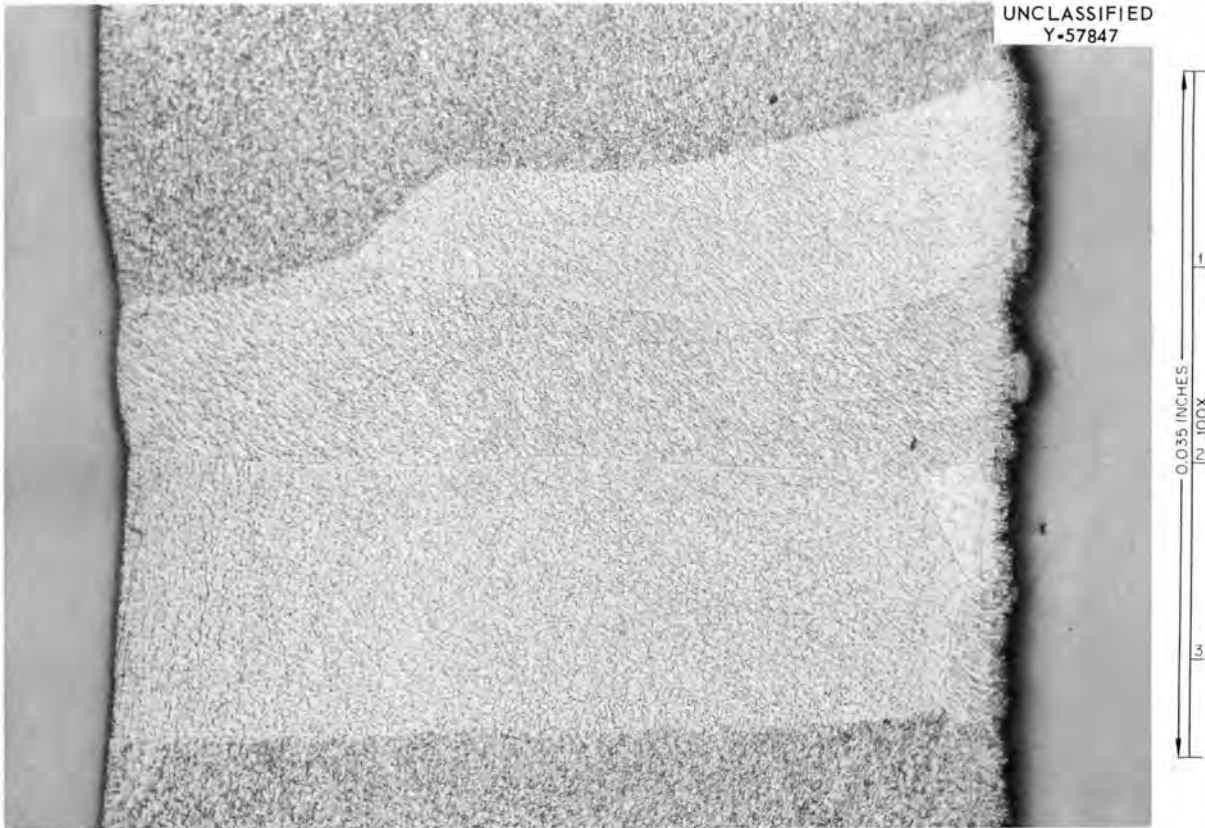


Fig. 1.2. UO_2 Dense, Uniform Deposit. Etched: 70 H_2O , 20 H_2O_2 (30%), 10 HNO_3 .

quite uniform at 400°C . Also, we have obtained uniform tubular deposits of pure tungsten at 500 and 600°C .³ In a continuing study of the effects of deposition conditions on homogeneity and uniformity, tungsten-rhenium alloy depositions have been conducted at 500 and 600°C .

Fifteen to forty times the stoichiometric amount of hydrogen required to reduce the tungsten and rhenium fluorides (WF_6 and ReF_6) was used in these codeposition experiments. The compound WF_6 was metered with a

³R. L. Heestand, J. I. Federer, and C. F. Leitten, Jr., Preparation and Evaluation of Vapor-Deposited Tungsten, ORNL-3662 (Aug. 1964).

Kel-F flowmeter, while ReF_6 was transferred to the reaction zone by three methods: (1) mixed with WF_6 and metered with a Kel-F flowmeter, (2) carried in a metered stream of hydrogen, and (3) metered directly with a mass flowmeter. The surface of the Kel-F in contact with the ReF_6 gradually darkened and was rendered useless. Both the carrier hydrogen method and the mass flowmeter required extensive calibration in order to determine the ReF_6 transfer rates; however, the mass flowmeter, being less sensitive to temperature and pressure fluctuations, was eventually adopted for metering the ReF_6 . In all experiments, the pressure was 10 torr.

Homogeneous deposits could not be consistently produced under the conditions used. The observation² that pure rhenium deposited non-uniformly at temperatures above 400°C was reflected in the nonhomogeneous rhenium content of most alloy deposits. This nonhomogeneity consisted of a higher rhenium content near the inlet to the reaction zone and indicates the relative ease of reduction of ReF_6 as compared to WF_6 . The feasibility of depositing homogeneous alloy, however, was indicated in an experiment conducted under the following conditions: 500°C temperature; $2000\text{ cm}^3/\text{min}$ hydrogen flow rate, including $25\text{ cm}^3/\text{min}$ as a carrier for ReF_6 ; $30\text{ cm}^3/\text{min}$ WF_6 flow rate; and 10-torr pressure. The rhenium content of this deposit varied with distance from the entrance of the reaction zone as shown below.

<u>Distance from Inlet of Reaction Zone (in.)</u>	<u>Rhenium Content (%)</u>
2	2
4	26
6	37
8	30
10	34
12	21

We cannot explain the reason for the alternately low and high rhenium contents. The section of the deposit between 5 and 11 in. from the inlet, however, averaged about 33% Re. Experiments are continuing to determine optimum conditions for homogeneity and uniformity.

Metallographic examination has not supported the previously reported observation² that the grain structure becomes less columnar with increasing rhenium content. Deposits containing from 4 to 46% Re had a columnar structure exhibiting only minor differences. No secondary phases (with the exception of a few minute precipitates) have been observed.

Rhenium deposition is being thermodynamically analyzed, and similar analyses for tungsten and tungsten-rhenium codeposition are planned. We have established computer programs to perform the numerous and laborious calculations that are required. These programs consist of free energy analyses for given initial conditions of reactions involving several possible end products and the equilibrium state existing among the products. In the rhenium program, for example, reactions between ReF_6 and hydrogen that lead to the formation of rhenium metal and the intermediate fluoride compounds ReF_5 , ReF_4 , and ReF_3 are being examined. These analyses are not expected to provide a fixed set of conditions for optimizing deposition of the metals or alloys but will indicate the general conditions of feasibility for each process. Even this limited information may narrow the wide ranges of variables (temperature, pressure, and composition of reacting gases) that should be explored.

Fabrication of Aluminum-Base Irradiation Test Plates

M. M. Martin W. J. Werner

In conjunction with the Phillips Petroleum Company, we have fabricated a series of aluminum-base miniature fuel plates to be used for determining the influence of high-temperature irradiation to high burnup on the dimensional and chemical stability of U_3O_8 and UO_2 dispersions. Four instrumented plates and thirty sample plates have been delivered on schedule to the ETR site for testing. Design specifications, which include materials, fuel loading, and dimensions, for the two types of plates were reported previously.⁴

⁴M. M. Martin and W. J. Werner, Fuels and Materials Development Program Quart. Progr. Rept. June 30, 1964, ORNL-TM-920, pp. 15-19.

The vast majority of our plates for irradiation met specification, even though the desired tolerances permitted little variations in core dimensions and ^{235}U content. In the instrumented plates, in which the fuel core consisted of two separate layers, we developed a frame design and fabrication procedure to diminish the longitudinal offset that develops between the two core layers during rolling. Initially, a solid plug of aluminum was inserted between the top and bottom fuel compacts and assembled into the machined cavity of a conventional picture frame. Instrumented plates that were roll bonded with this frame design exhibited an offset of about 0.61 in. of the top core relative to the bottom core. When the aluminum plug was designed to be integral with the frame (i.e., two shallow depressions to accept the compacts were machined in the top and bottom faces of the frame), the longitudinal offset was reduced from 0.61 to about 0.3 in. By placing the assembled billet on edge during preheating and reheating operations, we achieved an additional reduction in core offset to within the acceptable range of 0.1 to 0.2 in. This technique ensured a uniform temperature through the thickness of the billet and allowed equal amounts of work to be imparted to the top and bottom cores during rolling.

The control of variations in fuel loading, fuel homogeneity, and core-end effects were the principal problems encountered in fabricating the sample plates. The small core sections for the U_3O_8 plates were machined from master compacts and assembled in picture frames containing cavities with $1/32$ -in.-radius corners; the UO_2 cores and associated frame cavities were rectangular. As indicated in Table 1.2, the variations in effective and average core length and in ^{235}U content from core-weight calculations are within tolerance for the U_3O_8 plates. The plus and minus values are an estimate of the reproducibility of the process. We attribute the good dimensional control on core length and end effects of the U_3O_8 plates to the use of the $1/32$ -in.-radius corners. However, x-ray attenuation analyses of the ^{235}U content revealed excessive between-plate variations in fuel loading and showed the inherent inaccuracy of calculating uranium content on machined compacts from core weight. This error was accentuated in the UO_2 plates that contained spherical fuel particles of greater size and density; we found it necessary to

Table 1.2. Summary of Fabrication Parameters for HFIR-ATR Sample
Plates to be Irradiated in the ETR

	Core Composition, wt %	
	X8001 Al-41.9% U ₃ O ₈	X8001 Al-0.16% B ₄ C-55.7% Nb Coated (UO ₂ -ZrO ₂)
Specifications for core		
Length, in.	5.470 ± 0.061	5.470 ± 0.061
Width, in.	1.000 ± 0.031	1.000 ± 0.031
Thickness, in.	0.020 ± 0.003	0.020 ± 0.003
²³⁵ U content, g	2.205 ± 0.022	2.205 ± 0.022
Effective core dimensions		
Length, in.	5.520 ± 0.013	5.495 ± 0.076 ^a
Width, in.	1.009 ± 0.020	1.016 ± 0.020
Average core dimensions		
Length, in.	5.476 ± 0.030	5.377 ^a ± 0.105 ^a
Width, in.	1.001 ± 0.006	1.008 ± 0.006
Calculated thickness, in.	0.0203 ± 0.0006	0.0204 ± 0.0006
²³⁵ U content		
From core weight, g	2.192 ± 0.020	2.198 ± 0.020
From x-ray attenuation, g	2.213 ± 0.048 ^a	2.196 ± 0.024
Density		
Plate, g/cm ³	2.989 ± 0.078	3.256 ± 0.078
Core, g/cm ³	3.629 ± 0.035	4.504 ± 0.009

^aValue outside of specification.

Note: All plus and minus ranges calculated at the 95% confidence level to include 95% of the distribution.

press individual UO₂ compacts to adequately control the fuel loading of 2.205 ± 0.022 g ²³⁵U. The excellent reproducibility of 4.504 ± 0.009 g/cm³ for the density of the total core in the rolled UO₂ plates also indicates the control achieved. The distribution of the spherical particles in the core, however, remained more inhomogeneous than dispersions of equivalent uranium loading containing the finer U₃O₈ particles. We are presently studying blending to minimize localized fuel concentrations.

Hydrogen Absorption in the Water-Vapor Aluminum System

M. M. Martin

We are investigating hydrogen absorption by type 6061 and type 1199 aluminum to determine the influence of time, temperature, annealing-air dew point, and initial surface oxide thickness on the hydrogen content of the materials. Recent studies have centered on establishing a procedure for vacuum fusion analyses of internal hydrogen in aluminum, machining specimens to achieve minimum roughness, and installing two furnaces and associated equipment for reacting the specimens with airborne water.

In vacuum fusion analyses for internal hydrogen in unreacted material, we have found an erroneous contribution from surface water that is either absorbed in or combined with the surface oxide film. The hydrogen contents summarized in Table 1.3 for various experiments were determined on 0.625-in.-diam \times 1.500-in.-long slugs of pure aluminum. An elapsed time of either 3 or 21 hr occurred between machining the slugs from 3/4-in.-diam rods and vacuum fusion analyses. In comparing experiments 2 to 1, 7 to 3, and 9 to 8, the differences in the elapsed time revealed hydrogen changes of about 0.19, 0.04, and 0.15 cm³/100 g, respectively. We believe that only surface gas is indicated by the change, since hydrogen diffuses extremely slowly in aluminum at room temperature. Experiments 3 and 7 show the hydrogen content found after degassing the 3/4-in.-diam rod for 24 hr at 620°C at a pressure of less than 10⁻³ torr. The values of 0.11 and 0.15 cm³/100 g, however, still contain an unknown quantity of surface gas. Immediately prior to analyses, the slugs for experiments 5 and 6 were heated to 400°C for 4 hr at less than 10⁻² torr. The maximum internal hydrogen that could be removed by this treatment was calculated to be 0.02 cm³/100 g. The effect of degreasing the slugs in benzene before analyses is insignificant. Assuming that the 400°C heat treatment removed all of the surface gas, the internal hydrogen is estimated to be in the range of 0.02 to 0.05 cm³/100 g. The amount of surface hydrogen, therefore, is relatively large and estimated to be in the range of 0.1 to 0.2 cm³/100 g.

Table 1.3. Hydrogen Content of Type 1199 Aluminum Slugs After Various Treatments to Lower the Surface Gas

Experiment	Treatment	Elapsed Time (hr)	Hydrogen Content	
			(ppm)	cm ³ /100 g
1	Turned in lathe. About 0.062 in. removed from diameter.	3	0.29	0.35
2	Same as 1.	21	0.45	0.54
3	Degassed and turned.	3	0.094	0.11
4	Degassed and turned, followed by degreasing in cp benzene.	3	0.086	0.10
5	Degassed and turned, followed by heating to 400°C for 4 hr at < 10 ⁻² torr.	3	0.031	0.038
6	Degassed, turned, and degreased in cp benzene, followed by heating to 400°C for 4 hr at < 10 ⁻² torr.	3	0.017	0.021
7	Degassed and turned.	21	0.12	0.15
8	Degassed, turned, and degreased in cp benzene, followed by heating to 400°C for 1 hr at < 10 ⁻² torr.	21	0.035	0.042
9	Same as 8, followed by exposure to room temperature air for 21 hr.	21	0.16	0.19

Fabrication of Uranium Monocarbide with Fugitive Sintering Aids

J. P. Hammond

It is generally recognized that uranium carbide cannot be sintered to densities in excess of 93% of theoretical without using ultrapure atmospheric working conditions (as the British have used)⁵ or employing

⁵J. R. McLaren *et al.*, "The Sintering Behavior of Uranium Carbide," paper B12 at the Symposium on Carbides in Nuclear Energy, Harwell, England, Nov. 5-7, 1963.

sintering aids such as the much-referred-to-nickel addition.⁶ Where the latter approach is used, it is desirable to eliminate the additive constituent to avoid adverse effects such as weakening.

In the last report,⁷ we described two methods for fabricating uranium carbide with aids removable incident to the sintering process. The first used 5 to 10 wt % UAl_2 as the aid, and the aluminum was removed by volatilization during sintering under vacuum at only 1350°C. By picking up carbon made available from the graphite firing crucible, we obtained stoichiometric composition with density in excess of 97% of theoretical. The second method used 0.5 to 0.75 wt % UBe_{13} as the additive and sintering was done in vacuum at 1525°C in a tungsten-lined tantalum crucible. Here, the sintering aid was dissolved in the matrix phase and stoichiometric carbide with densities around 95% of theoretical were achieved. Pure carbide was used as a charge material (nonconsumable arc melted) in order to better study the processes involved. Sintering with UAl_2 was seriously impaired either by using impure UC as starting material, such as high-oxygen-containing UC derived from UO_2 by graphitic reduction, or by incorporating excess carbon in the carbide charge.⁸ The effects of these two variables on the fabrication results using UBe_{13} as the sintering aid are illustrated in Tables 1.4 and 1.5. The sintering temperatures and amounts of UBe_{13} used are near optimum.

High oxygen or above-stoichiometric carbon in the charge severely penalizes the densification. In the case of sintering with UAl_2 , the low densification associated with excess carbon in the charge was

⁶K. M. Taylor *et al.*, "Sintering Characteristics of UC and (U,Pu)C With and Without Small Additions of Nickel," paper B8 at the Symposium on Carbides in Nuclear Energy, Harwell, England, Nov. 5-7, 1963.

⁷J. P. Hammond, Fuels and Materials Development Program Quart. Progr. Rept. June 30, 1964, ORNL-TM-920, pp. 19-22.

⁸J. P. Hammond and G. M. Adamson, Jr., "Fabrication of Uranium Monocarbide with a Volatile Sintering Temperature Depressant," paper B15 at Symposium on Carbides in Nuclear Energy, Harwell, England, Nov. 5-7, 1963.

Table 1.4. Effect of Carbide Purity on Fabrication
Results with the UBe_{13} Sintering Aid

Pellet Number ^a	UC Type	Amount UBe_{13} (wt %)	Sintering Temperature (°C)	Theoretical Density (%)	
				Green	Fired
UC-21 11	Arc-cast ^b	0.75	1525	65.0	95.2
UC-21 12	Arc-cast ^b	0.75	1525	65.0	94.8
UC-20 99	Y-12 ^c	0.75	1525	64.8	77.1
UC-20 100	Y-12 ^c	0.75	1525	64.8	77.0
UC-20 25	Arc-cast ^b	0.50	1500	67.0	95.0
UC-20 26	Arc-cast ^b	0.50	1500	67.0	95.0
UC-20 29	Y-12 ^c	0.50	1500	62.4	83.2
UC-20 30	Y-12 ^c	0.50	1500	62.3	83.4

^aPellets of 0.50-in. diam, 2 wt % camphor, 25-tsi pressing pressure, vacuum sintered in tungsten-lined tantalum crucible.

^bArc-melted from high-purity elemental ingredients.

^cGraphite-reduced from UO_2 ; composition after grinding was 4.74% C, 0.070% O.

Table 1.5. Effect of Carbon Level of UC Charge on Sintering
Results for UC-0.75% UBe_{13} at 1525°C

UC-21 Pellet No. ^a	UC Carbon Level (wt %)	Theoretical Density (%)	
		Green	Fired
9	4.7	67.3	92.4
10	4.7	67.0	92.8
11	4.8	65.0	95.2
12	4.8	65.0	94.8
13	4.9	66.0	86.7
14	4.9	66.1	86.6
15	5.1	68.2	75.7
16	5.1	68.3	75.7

^aPellets of 0.5-in. diam pressed at 25 tsi with 2 wt % camphor, vacuum sintered in tungsten-lined tantalum crucible. UC charges arc-melted from high-purity elementals.

explained on the following basis.⁸ The excess carbon, whether as UC_2 or U_2C_3 , thwarted sintering by reacting with the uranium-rich liquid phase (formed as aluminum is removed) as quickly as it was formed. Thus, the benefits of sintering in the presence of a grain-wetting liquid phase could not be realized. However, some assistance to densification in the hyperstoichiometric composition was attributed to the presence of a reactive aluminum vapor phase that scavenged the powders of oxide films that were responsible for inhibiting sintering. We believe that the deleterious effect of oxygen on densification is associated with the carbon effect. Oxygen atoms substitute for carbon in the carbide lattice ($UC_{1-x}O_x$), freeing carbon to form U_2C_3 .⁹ The fabrication results shown in Tables 1.4 and 1.5 suggest that the same mechanisms may be at play in the UC- UBe_{13} system.

Using U_3Si_2 as the sintering aid with arc-cast carbide of high-purity as the charge material, we obtained excellent results with 1.5 and 2.0 wt % additive when sintering in vacuum at 1550°C — theoretical densities were around 97%, and the structures were virtually free of secondary constituents. Chemical analyses indicated, as in the case of the beryllide sintering, that the major portion of the additive was dissolved in the carbide phase.

Further tests were conducted on silicides as sintering aids using a high-oxygen-containing grade of carbide as the charge, a material prepared from UO_2 by graphitic reduction. Extraordinarily good densification occurred in spite of the low purity of the charge. It can be seen in Table 1.6 that U_3Si_2 gave the best results of the silicides examined, giving a high density (97% of theoretical) for a 1600°C sintering temperature. In these tests, a small amount of UBe_{13} was incorporated in the crucible, external to the pellets, to create a slight vapor of beryllium for scavenging the carbide powder of sintering-inhibiting oxide films.

⁹N. H. Brett *et al.*, "The Substitutional Solubility of Oxygen in UC, $(U_{0.85}Pu_{0.15})-C$ and PuC ," paper A12 at Symposium on Carbides in Nuclear Energy, Harwell, England, Nov. 5-7, 1963.

Table 1.6. Preliminary Results on UO_2 -Derived Uranium Carbide Using Various Silicides as Sintering Aids at $1600^\circ C^a$

UC-22 Pellet No. ^b	Additive (wt %)	Theoretical Density (%)	
		Green	Fired
7	1.50 U_3Si_2	67.5	97.0
8	1.50 U_3Si_2	67.5	97.0
9	0.75 Y_4Si_3	67.1	93.2
10	0.75 Y_4Si_3	67.5	93.2
11	1.50 USi	67.6	94.4
12	1.50 USi	67.5	94.2

^aSalt for vapors, 0.25 UBe_{13} .

^b0.50-in. pellet, 2 wt % camphor, 25-tsi pressing pressure, vacuum sintered in tungsten-lined tantalum crucible; and UC charge = 4.74% C, 0.70% O.

Future studies will be directed primarily at sintering with the silicide aid and determining the effects of fabrication variables on final chemistry.

2. NONDESTRUCTIVE TEST DEVELOPMENT

R. W. McClung

Our program is intended to develop new and improved methods of evaluating reactor materials and components. To achieve this we are studying various physical phenomena, developing instrumentation and other equipment, devising application techniques, and designing and fabricating reference standards. Among the methods being actively pursued are electromagnetics (with major emphasis on eddy currents), ultrasonics, and penetrating radiation. In addition to our programs oriented toward the development of methods, we are studying these and other methods for evaluation of problem materials and developing techniques for remote inspection.

Electromagnetic Test Development

C. V. Dodd

S. Aveyard¹

We have continued research and development on electromagnetic phenomenon on both an analytical and an empirical basis. As part of the program we are studying the mathematical determination of impedance of an eddy-current coil and other electromagnetic field parameters as a function of coil dimensions, frequency, specimen conductivity and permeability, and coil-to-specimen spacing or "liftoff". The relaxation techniques² allow the solution of the electromagnetic boundary value problem on a digital computer. The differential equations for the field are approximated by finite difference terms. By making a number of correcting calculations the values of the field can be made to converge to agreement with the differential equations at every point. Several of the finite difference equations when applied to problems with large permeability variation caused an over correction and a nonconverging oscillating solution. To overcome this, a new

¹On loan from AERE, Harwell, England.

²C. V. Dodd, Fuels and Materials Program Quart. Progr. Rept., June 30, 1964, ORNL-TM-920, pp. 37-40.

relaxation equation that converges to the correct solution for simple one-dimensional cases has been written and tested and is now being incorporated into the computer program. Because of the cost of computer operation, further changes are being made in the program to decrease the running time.

We are continuing development on the phase-sensitive eddy-current instrument conceived and developed at ORNL.³ This device offers several advantages over other eddy-current equipment including relative insensitivity to "liftoff", linearity of response for through-transmission operation, and the ability to examine thicker material sections. These capabilities are achieved through monitoring the phase shift of the electromagnetic wave rather than measuring the amplitude changes of the coil. The operating frequency of the instrument was too low to resolve the reflected signals from thin sections of low-resistivity materials when using the very miniature coils necessary for small area interrogation. Therefore, new plug-in circuit boards have been designed and constructed which operate at a frequency of 2 Mc. The principal application of this system has been for thickness measurements or the detection of large flaws. Signals from small discontinuities were generally hidden in the larger signals due to dimensional variations. Two approaches are being followed to increase the sensitivity to small flaws.

We have designed and built time differentiating circuits that selectively amplify rapidly changing signals from discontinuities without affecting the slow changing signals from dimensional variations. Successful utilization of the new circuits require constant speed inspections but an increase of 10 or more has been seen in the sensitivity to defects. In order to achieve this greater sensitivity to flaws when performing manual inspections, we have constructed a hand-held probe which vibrates at a fixed frequency. We shall determine its optimum frequency and amplitude of vibration.

³C. V. Dodd, "Application of a Phase-Sensitive Eddy-Current Instrument," Mater. Evaluation 22(6), 260 (1964).

A common inspection problem in clad structures such as fuel elements is the measurement of cladding thickness. Assurance must be made that variations in core thickness or cladding thickness on the opposite surface do not affect the measurement. A series of measurements were made to check the applicability of the phase-sensitive instrument to such a problem. The arbitrarily chosen samples were 0.065- and 0.052-in.-thick cores of 1100 aluminum that were "clad" on either side with shims of copper. With a 200-mil-diam coil and an operating frequency of 10 kc, copper clad thickness measurements were made accurately to within 1 mil of the true 10- to 19-mil value with no visible influence as a function of varying core thickness or variation in cladding on the opposite surface. It is interesting to note that the conductivity ratio between the cladding and core materials was less than the 2:1 value which had been considered minimum for accurate cladding thickness measurements.

Ultrasonic Test Methods

K. V. Cook R. W. McClung Sydney Aveyard¹

We have continued our studies on the behavior of ultrasound in thin sections with the principal effort being the detection of nonbonds in cladding structures. The through-transmission ultrasonic method has been used successfully to detect nonbonds in thin fuel plates by monitoring changes in transmitted intensity due to nonbonds. A problem with such a system is the possible presence of other conditions in the fuel plate causing ultrasonic attenuation that would be erroneously interpreted as a nonbond. An area in which this could be of more concern is for the detection of nonbond in aluminum-clad dispersion-core fuel plates. Our work on such plates with dispersions of U_3O_8 , UAl_3 , and niobium-coated UO_2 has indicated that the UAl_3 dispersion cores have shown very little variation in attenuation, enhancing reliable inspection. The oxide cores have higher and more variable attenuation. One source of this variation is related to the final shape of the stringered fuel particles. We have shown the highest attenuation variation to be due to laminar stringering in both transverse and longitudinal directions produced during fuel plate fabrication. This will tend to reduce the nonbond sensitivity which can be expected or it will increase the spurious rejection rate.

A common technique for manufacturing reference nonbonds in a plate standard is to drill holes with a flatbottom parallel to the major surface. An alternate standard has been developed with holes drilled parallel to the surface before rolling the plate to final thickness. This produced laminations at different depths. Similar response from each defect indicated that the through-transmission ultrasonic technique is not very sensitive to depth location. This could not be adequately demonstrated with the flatbottomed holes because of the secondary effect of varying length of the sides of the holes.

Since through-transmission techniques are not amenable to all non-bond evaluation problems, two-crystal reflection and Lamb-wave techniques are often required. The latter techniques require the establishment of appropriate inspection angles and frequencies, and we have designed and fabricated a two-crystal angle manipulator.⁴ This device, because of the precision control and reproducibility of incident points and angles, should facilitate experimental determinations and improve data reliability in the study of variation of ultrasonic reflection, transmission, and Lamb-wave generation in thin or clad sections. A preliminary series of Lamb-wave experiments have been conducted to test the usefulness of the newly designed and fabricated two-crystal angle manipulator. A variable frequency oscillator was used as the ultrasonic generator. Accurate angle positioning was achieved as evidenced by very good correlation between experimental results and theoretical Lamb-wave modes despite the fact that the modes are efficiently generated over a very narrow angle range. We found that the micrometer adjustment of the distance between transmitting and receiving probes is quite useful for quantitative measurement of attenuation of the Lamb waves. However, a few minor changes in the system are desirable. Improvements are needed in the sample positioning for the best reproducibility. The quartz crystals that are being used limit the useful bandwidth of the system to about ± 1 mc of the fundamental and third harmonic frequencies. A better baffle system is needed to block direct reflection from the specimen surface.

⁴K. V. Cook and R. W. McClung, Fuel and Materials Development Program Quart. Progr. Rept., June 30, 1964, ORNL-TM-920, pp. 40-42.

We are continuing to work on the problems encountered in tubing inspection. A major problem is the establishment of realistic ultrasonic notch standards for calibration. Electrical discharge machining appears to be a reliable method for making both inner- and outer-surface notches, but we are having difficulty in obtaining reproducible notches. Very shallow (0.001-in. deep) notches have rounded bottoms; and as can be seen in Fig. 2.1, there is no component of the notch perpendicular to the surface — a condition for optimum reflection. Because of this we have shown that smaller, perpendicular flaws will produce signals equal to those from these notches. A laboratory-model electrical-discharge machine has been ordered, and delivery is expected in October. This should enable us to resolve some of these problems and establish a more consistent fabrication practice.



Fig. 2.1. Cross Section of 0.001-in.-Deep Notch Produced by Electrical Discharge Machining in Wall of Tube. As polished.

Penetrating Radiation

Gamma Scintillation Gaging - B. E. Foster and S. D. Snyder

We are continuing the application of x- and gamma-ray attenuation to the evaluation of fuel elements. Variation in transmitted intensity can be monitored readily by scintillation gaging and can be related through proper calibration to the fuel content within the area of the radiation beam. Recent work has been directed toward measurements of ultimate sensitivity of this type system and application of the method for the determination of total fuel content within a fueled configuration. This latter consideration is quite important because of the need to know total fuel quantities from both criticality and accountability standpoints. The preliminary experiments to determine total fuel content were performed on 18 irradiation test plates fabricated at ORNL. Ten of the specimens contained U_3O_8 -Al dispersion cores with aluminum cladding. The remaining eight specimens were niobium-coated UO_2 - ZrO_2 particles dispersed in aluminum with aluminum cladding. Calibration curves (milligram uranium vs chart reading) were obtained for each of the above types of fuel plates using chemistry determinations on scanned sections in conjunction with the calibration curve previously developed for HFIR fuel plate homogeneity evaluations. The technique which we are using required multiple scans on the fuel plate, determination of average scan values, planimeter measurement of the projected fuel area, and calculations using the various determined values. The average deviation of the experimentally determined fuel content from the actual core loading content was less than 0.5%.

Our measurement of maximum sensitivity was made to determine the minimum specimen thickness change and the minimum radiation intensity change that could be detected above the background noise level. When operating under conditions similar to that recently used for homogeneity determination in HFIR- and ATR-type fuel plates, thickness changes and intensity changes of about 0.2% were detected at a signal-to-noise ratio of 2:1. These values will facilitate subsequent calculations of system capability for specific material evaluations using theoretical mass attenuation coefficients.

X-Ray Imaging with Closed-Circuit Television - W. H. Bridges

There are a number of applications in which an x-ray sensitive, closed-circuit television system could provide information that would otherwise be difficult or impossible to obtain. One such application is the measurement of fuel expansion inside a metal tube as a function of rapid temperature changes. The general features of the experimental setup were described last quarter.⁵ The specimen is heated by direct current resistance heating of a central rod. The > 500-amp current establishes an intense magnetic field, upsets the camera focusing, and severely distorts the TV picture. Enclosing the Vidicon camera in a soft iron box improved the "on" cycle. The camera originally used permanent magnets for focusing, but conversion to electromagnetic focusing further improved the image. We built several different focusing coils and found that a tapered field coil performed best; however, there is still distortion of the image when the power is on, but the image is sufficiently clear to show the motion of the specimen.

Inspection Development of Problem Materials

K. V. Cook

R. W. McClung

We have continued to work on nondestructive tests for unusual materials that are difficult to inspect and on new materials that have no evaluation history. This has included such items as graphite and refractory metals including tantalum-, molybdenum-, and niobium-base alloys. We found that conventional penetrant, radiographic, and ultrasonic techniques could be applied to D-43,⁶ T-111, and B-66 alloy tubing. Excessive "noise" levels have been encountered with eddy-current encircling coil examinations, particularly on very thin wall tubing. We believe much of the latter to be associated with localized dimensional variations.

⁵W. H. Bridges, Fuel and Materials Development Program Quart. Progr. Rept., June 30, 1964, ORNL-TM-920, pp. 44-46.

⁶R. W. McClung and K. V. Cook, Nondestructive Evaluation of D-43 Alloy Tubing by Oak Ridge National Laboratory, ORNL-TM-843 (June 1964).

3. SOLID REACTION STUDIES

T. S. Lundy

Our purpose is to provide information concerning solid-state reactions of importance in the development of materials for high-temperature application. We are emphasizing the study of mechanisms of these reactions by measuring diffusion rates in the solid state by various methods. In particular, we are studying the diffusion rates in various body-centered cubic refractory metals over wide ranges of temperatures.

During this quarter, we have concentrated on measuring diffusion coefficients for ^{95}Nb in tantalum single crystals and have written a paper covering this work. This paper is being included as our contribution to this report.

Diffusion of Nb^{95} Into Tantalum Single Crystals*

R. E. Pawel and T. S. Lundy

Introduction

Several recent investigations¹⁻⁵ have indicated that diffusion from a plane source into a metal does not necessarily result in an ideal Gaussian penetration curve. These results commonly show a decrease in the apparent diffusivity in the near-surface region; this type of behavior is, perhaps, common to a much larger number of diffusion investigations than is generally realized, being subtly suggested by the fact that the first point or two of the penetration plot is high compared to the remainder of the data, and sometimes being observed only when the sectioning process is continued to great depths. A similar type of penetration has been observed for diffusion into intermetallic compounds⁶ and ceramic bodies.⁷ Such characteristics have been subject to a number of interpretations and it is doubtful that a single explanation is applicable to all cases.

Since diffusion behavior of this type has many implications from the standpoint of both diffusion studies and surface studies in general, it is important to establish for each individual case whether: (1) the so-called near-surface region is "real", indicating a diffusion constant

*Paper accepted for publication in Acta Metallurgica.

that is either a function of depth or the result of the addition of two constants from different mechanisms, or (2) if it occurs as a result of an artifact such as (a) a surface film or diffusion barrier, (b) an impurity induced during the deposition or diffusion of the isotope, (c) a failure to meet the necessary boundary conditions for the mathematical treatment, or (d) an anomaly associated with the method of sectioning. Until recently, because of a lack of sufficiently sensitive experimental procedures, only cursory attention has been given to the questions posed above.

This paper presents some comparatively low-temperature data on the diffusion of Nb⁹⁵ into single crystals of tantalum where the behavior described above is quite apparent. The anodic film sectioning technique previously described^{4,5} was used to construct the penetration curves. The technique was developed primarily for the study of diffusion behavior at low temperatures, which automatically places importance on the consideration of near-surface effects.

Experimental Procedure

Tantalum specimens were cut from approx 1/2-in. single-crystal rods to form cylindrical disks about 1/4 in. long. One face of each disk was prepared by standard metallographic techniques, finishing with a 1-hr electropolish in a 90% H₂SO₄-10% HF solution. It was necessary to obtain a smooth, scratch-free surface at this point in order to insure optimum sectioning conditions later in the process.

The key to the successful use of the anodic film method of sectioning, in terms of both the experimental aspects and the mathematical interpretation, lies in obtaining a very smooth initial surface which is not appreciably disturbed by the application of the isotope or the ensuing diffusion anneal. Most of the data presented in this paper were taken from specimens on which the isotope was deposited as a dilute oxalate solution.⁴ However, in order to further test this part of the experimental procedure, electrolytic and vapor deposition methods were also used. The vapor deposition method proved to be superior, especially for diffusion experiments at temperatures below 1200°C. In all cases, rough calculations indicated that less than a

monolayer of active isotope was deposited on the surface. However, the isotope undoubtedly was distributed in a layer of impurities and daughter elements which had an average thickness somewhat larger but difficult to estimate. The effect of these impurity elements upon the near-surface diffusion characteristics may be an important one and is discussed in a later section.

After the diffusion anneal, the specimens were sectioned by the anodic film method. Anodization was conducted in a 0.2% KF solution, and the films stripped onto plastic tape in the manner previously reported.^{4,8} The section thickness was varied between 130 A and 650 A depending upon the diffusion treatment. The isotope concentration in each stripped film was determined in a gamma-counting facility consisting of a single-channel analyzer using a 3 x 3-in.-NaI (Tl) scintillation crystal in a lead container.

Results and Discussion

Penetration curves for the diffusion of Nb⁹⁵ in tantalum single crystals were obtained at several temperatures from 1050 to 1600°C. Generally, the curves, plotted as $\ln A$ vs x^2 , (where A is the specific activity and x the penetration depth) did not have a constant slope. At sufficiently large penetration depths, depending upon the annealing treatment, the slope of the curve decreased appreciably. While in many instances, especially for the higher temperature experiments, an adequate representation of the data was two straight lines on the $\ln A$ vs x^2 plot, the exact analytical form of the activity profile at large penetration depths was not obvious, at least partly because of the small amount of activity present in the deeper region. Thus it was difficult to ascertain, on the basis of a single penetration curve, which segment reflected normal, "bulk" diffusion behavior.

Figure 3.1 illustrates penetration behavior typical of that obtained in the intermediate temperature ranges. In this particular case, the specimen was annealed for 5.02 hr at 1358°C with both Nb⁹⁵ and Ta¹⁸² tracers which enabled a direct comparison to be made between their penetration characteristics. The two parts of the penetration curve are evident from the figure and the apparent diffusion coefficients

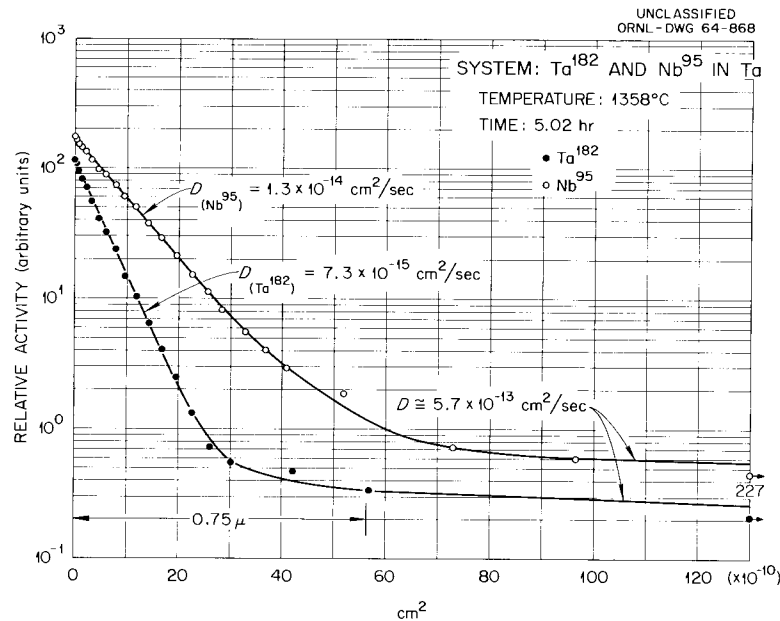


Fig. 3.1. Activity Profiles for Diffusion of Nb^{95} and Ta^{182} into Tantalum Single Crystals after 5.02 hr at 1358°C .

for each region are listed for both diffusing species. Note that the coefficients differ by approximately a factor of two (at least in the near-surface region) for the diffusion of the two isotopes. A comparison of such values with those previously reported for self-diffusion in tantalum⁹ and for the diffusion of niobium in tantalum¹⁰ in this temperature range (presumably "bulk" diffusion) suggested that it was the second, or deeper, region which represented bulk diffusion behavior. However, a critical evaluation of the data to be described here for diffusion in this system permitted bulk behavior to be ascribed to the near-surface region. The second region was associated with the contribution to the total penetration profile of a second diffusion mechanism, presumably diffusion down short-circuit paths such as dislocation pipes. The contribution of such paths, especially at low temperatures has been both predicted and observed by several investigators.^{2, 11-13} In order to reach such a conclusion, it was necessary to examine the data in terms of the experimental and analytical procedures as well as its behavior as a function of several experimental variables.

Analytical Procedure. - For diffusion experiments utilizing radioactive tracers, one particular solution to the diffusion equation

results from the imposed initial and boundary conditions. Usually, choosing the proper solution is not difficult. However, when dealing with very small penetration distances, the choice is not a straightforward one because of difficulties in adequately defining the system in terms of idealized mathematical requirements. It is important that the experimental and mathematical descriptions be mutually consistent.

If a thin layer of radioactive isotope of finite thickness h and specific activity A_0 is deposited on the surface of a semi-infinite homogeneous specimen, the solution to Fick's second law for unidirectional diffusion yields:

$$A_{(x,t)} = \frac{A_0}{2} \left[\operatorname{erf} \frac{h-x}{2\sqrt{Dt}} + \operatorname{erf} \frac{h+x}{2\sqrt{Dt}} \right] \quad (1)$$

where: $A_{(x,t)}$ = The activity at a distance x into the specimen at time t ,

x = total penetration depth, including isotope layer,

D = the diffusion coefficient, and

t = the annealing time.

If the isotope layer, h , is sufficiently thin, (a frequently used criterion is that $h < 0.1\sqrt{Dt}$), the solution for a "plane source" is applicable. In this case

$$A_{(x,t)} = \frac{M}{\sqrt{\pi Dt}} \exp \left(-\frac{x^2}{4Dt} \right) \quad (2)$$

where: M = the total activity per unit area in an infinitesimally thin isotope layer at $x = 0$, $t = 0$.

For the case of most diffusion investigations in which the sectioning of the specimen is performed by lathe-machining or grinding, it is desirable that \sqrt{Dt} be made comparatively large in order to preclude effects due to the finite thickness of the sections as well as the isotope layer. For example, Shirn, et al.¹⁴ have shown that the usual working form of Eq. 2 should include the section thickness, δ , as a variable so that

$$\frac{d \ln A_{(x,t)}}{d(x^2)} \approx -\frac{1}{4Dt} \left[1 - \frac{\delta^2}{24Dt} + \dots \right]. \quad (3)$$

Thus, in order to apply Eq. 2 directly, it is necessary that $\delta \lesssim 1.5\sqrt{Dt}$ so as to limit errors in the experimental values of the diffusion coefficient to less than 10%. As has been pointed out previously,¹⁵ a consideration of this correction as well as that due to section misalignment, is all too often neglected, and in such cases the measured diffusion coefficients will be too large.

Mortlock¹⁶ has recently emphasized that an often overlooked requirement for the direct use of the above equations is that the surface concentration of the isotope must drop below the solubility limit in a time that is short compared to the total annealing time. Thus, for systems where the solubility of the isotope is small, a careful inspection of this potential source of trouble is necessary. For the case of an infinitesimally thin layer diffusing into a specimen under the condition that the surface concentration does not change with time, Mortlock showed that the apparent diffusion coefficient determined by Eq. 2 decreases rapidly for $x < \sqrt{Dt}$. In the system presently under investigation, the solubility of the isotope is large; however, because the isotope layer is not pure, it is necessary to consider the possibility that a diffusion barrier or its equivalent could exist which could lead to results similar to those where solubility conditions controlled.

Evaluation of the Present Method. - The study of diffusion phenomena at low temperatures places rather severe practical limitations on the penetration distances and, consequently, more restrictions are necessary concerning the thickness of the isotope layer, h , and the sectioning thickness, δ , if Eq. 2 is to be used directly. Since the experiments considered in this paper involved small penetration distances as well as very small section thicknesses, particular attention has been paid to these quantities to ascertain insofar as possible if the observed penetration behavior could have been seriously influenced by a failure to meet experimentally these necessary conditions.

The sensitivity of the anodic film sectioning procedure would, for a one-day diffusion anneal, permit accurate determinations of diffusion coefficients as low as about 10^{-17} cm²/sec. However, the strict use of Eq. 2 at this extreme apparently requires that the thickness of the initial isotope layer be less than 100 Å. The extent to which a thicker

isotope layer would affect the computed diffusion coefficients (determined from a plot of $\ln A$ vs x^2) is difficult to estimate for all cases; however, for values of \sqrt{Dt} as small as 3×10^{-6} cm, for example, the deviations from "plane layer" behavior can be shown to be small for layer thicknesses of at least 1000 Å. In addition, the existence of thick isotope layers results in a concave downward segment of the $\ln A$ vs x^2 plot near $x = 0$. This behavior is opposite to that observed in the region under consideration.* Thus, the present experimental procedure appears to meet satisfactorily the boundary conditions necessary for the direct use of Eq. 2 with the possible exception of the existence of a diffusion barrier. However, if a diffusion barrier or other discrete layer remained on the surface of the specimen after the diffusion-anneal, the associated change in the anodizing characteristics would undoubtedly have been recognized. For annealing temperatures above 1200°C, problems of this sort were not serious, although at lower temperatures short-time anneals sometimes failed to absorb completely patches of the isotope layer originally deposited as a solution. Vapor deposition of the isotope appeared to reduce this difficulty significantly. It should also be pointed out that it is not necessary for the isotope to be deposited uniformly over the whole surface from which diffusion occurs,¹⁷ but only that it be "thin" at all points where it does exist.

Consequently, for the above reasons, the near-surface behavior in this system is argued to be an intrinsic property and not a result of a failure of the experimental procedure to meet the required boundary conditions.

*The concave downward behavior results when the outer surface of the isotope layer is considered $x = 0$. For the case of the original metal surface being considered $x = 0$, which is the limiting value if the layer is subject to anodic dissolution during the formation of the first anodic film, it is possible in some instances to account for slightly concave upward behavior near $x = 0$. However, for a layer thickness of 1000 Å, the extent of the upward curvature is negligibly small compared to that actually observed. In addition, observations of the specimen during anodization indicate that the anodic dissolution of a superficial layer of this sort is not an important process.

Evaluation of the Data. - The results of two sets of experiments led to the conclusion that the first portion of the penetration curve was associated with bulk diffusion. Basically, diffusion in this region was insensitive to changes in the initial state of the surface as well as the structure of the specimen, whereas diffusion in the second region was highly sensitive to the crystalline perfection.

The reproducibility of the apparent diffusion coefficients in the first region of the penetration plot is illustrated in Fig. 3.2 which shows the near-surface penetration behavior for Nb^{95} in tantalum single crystals as a function of time at 1350°C . For the time intervals involved, 0.5, 2, and 8 hr, the initial portions of the curves were adequately represented by straight lines from which the apparent diffusion coefficients were satisfactorily reproduced. Similar results were obtained on a series of single-crystal specimens annealed at 1250°C . The diffusion coefficients associated with the near-surface region were also reproduced for both different batches of isotope and different deposition techniques as well as for different furnace atmospheres (vacuum and argon) during annealing.

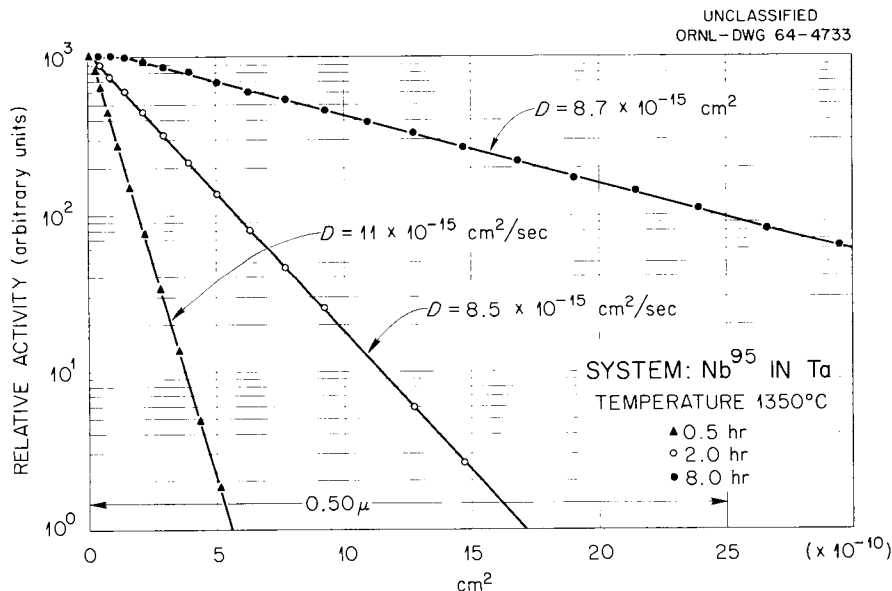


Fig. 3.2. Activity Profiles for Diffusion of Nb^{95} into Tantalum Single Crystals after Diffusion at 1350°C for 0.5, 2.0, and 8.0 hr. (Only first portion of activity profile illustrated.)

The structure sensitivity of the diffusion profile is illustrated in Fig. 3.3 which compares the penetration curves for diffusion of Nb^{95} into single crystal and polycrystalline tantalum after identical treatments. The polycrystalline specimen in this case had a strong (110) texture, but no attempt was made to characterize it further. As is evident from the figure, the distinguishing difference was associated with the relative importance of the deeper region. The penetration plot for the single crystal remained linear for about four decades of activity while that for the polycrystal "tailed-off" quickly into a long, relatively high-activity curve which was not precisely linear when plotted as $\ln A$ vs either x^2 or x .¹⁸ A self-consistent explanation for the observed behavior is that the deeper region resulted from activity contributions due to diffusion of the isotope down high-diffusivity paths. The effective density of these paths was comparatively high in the case of the polycrystalline specimens but not completely absent in the single crystals. X-ray measurements confirmed the fact that the single crystals used in this investigation actually consisted of arrays of subgrains; these boundaries would be capable of serving as regions of high diffusivity. A micrograph of an appropriately decorated single crystal is shown in Fig. 3.4. The small-angle boundaries were delineated by the dark oxide platelets formed during gaseous oxidation of the electropolished tantalum.¹⁹ Hence, the near-surface region, whose behavior was affected only slightly by structure, is logically associated with the lower mobility lattice (or bulk) diffusion with the appropriate coefficients determined directly from Eq. 2.

These results emphasize the fact that it is difficult to obtain measurements of bulk diffusion coefficients at low temperatures using polycrystalline specimens, since the structure sensitive contribution to the overall activity in this case is considerable - even in the extreme near-surface region.

The bulk diffusion coefficients obtained thus far in the investigation are plotted in the customary fashion in Fig. 3.5. For comparison, the data of Peterson¹⁰ and of Gruzin and Meshkov⁹ are also presented. Although the present work is being continued to both higher and lower temperatures in order to define the curve more accurately,

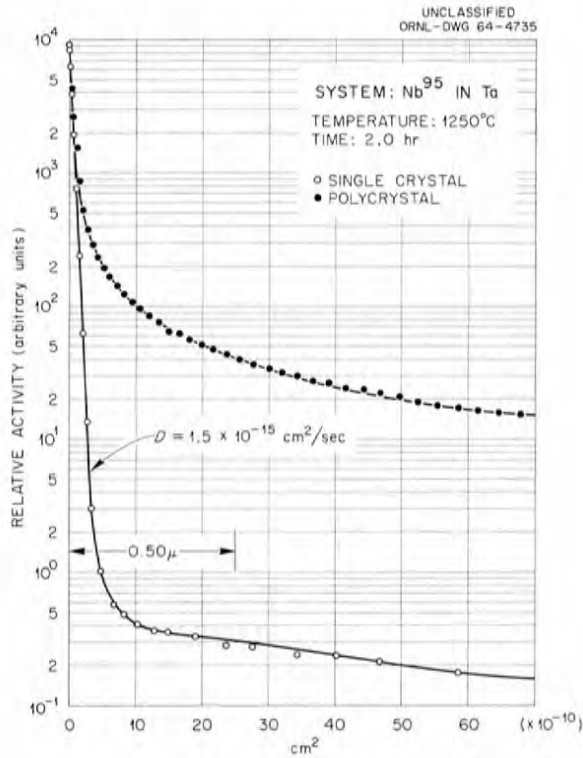


Fig. 3.3. Activity Profiles for Diffusion of Nb⁹⁵ into Tantalum Single Crystal and Tantalum Polycrystal Specimens after 2.0 hr at 1250°C.



Fig. 3.4. Photograph of Decorated (Lightly Oxidized) Tantalum Single Crystal Showing Large Subgrains.

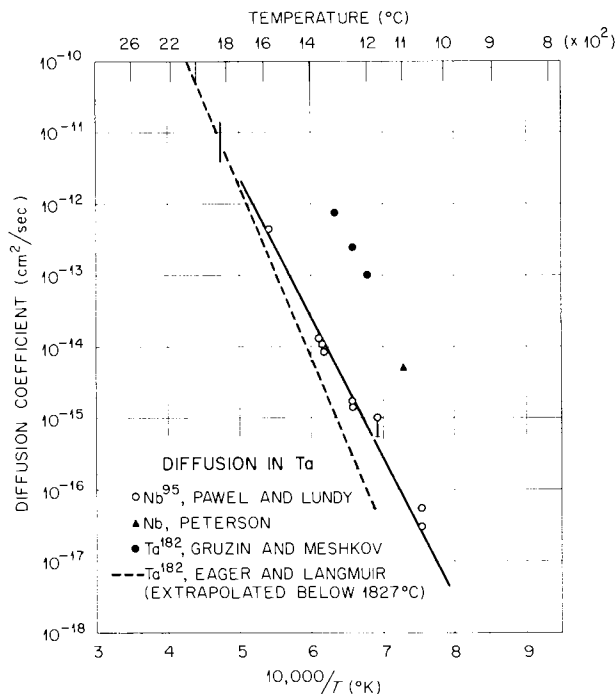
UNCLASSIFIED
ORNL-DWG 64-4732

Fig. 3.5. Diffusion in Tantalum. A comparison of the measured diffusion coefficients with those from other investigations. The data of Eager and Langmuir are extrapolated below the solid bar drawn at 1827°C.

the present data is adequately described by the straight line drawn on the figure. Within this temperature range the data are represented by the parameters $Q \cong 90$ kcal/mole and $D_0 = 0.02$. The agreement with the results of the previous investigators who worked in this same temperature range is not good, as was mentioned previously. However, if the data of Eager and Langmuir²⁰ for self-diffusion in tantalum from 1827 to 2527°C are extrapolated (dashed line in Fig. 3.5), a much better agreement exists. In fact, if the Eager and Langmuir curve is shifted upward by a factor of two — the approximate difference in the diffusivity of Nb⁹⁵ and Ta¹⁸² in tantalum — the agreement is striking. The high-temperature measurements of Eager and Langmuir were undoubtedly bulk diffusion measurements (indeed, they made note of the "much more rapid grain-boundary diffusion near 1550°C"). Therefore, it appears that the profiles obtained by Gruzin and Meshkov and by Peterson were

subject to misinterpretation in that within the sensitivity of their measurements, the slopes of their penetration plots were primarily determined by grain boundary or other short-circuit mechanisms rather than by bulk diffusion. It is significant to observe that the apparent diffusion coefficients determined from the second region (see Figs. 3.1 and 3.3, for example) for either single or polycrystal specimens agree well with their data.⁴ Thus, it is apparent that data for diffusion at low temperatures must be interpreted carefully even when single crystals are used.

As indicated earlier in this paper, it is impossible to generalize from the present results to the results of all investigations where non-Gaussian behavior has been observed. Certainly the possibility exists that an anomaly in the penetration profile may arise from several causes, and it is necessary for such behavior to be examined from as many angles as possible in order to select the most probable mechanism. The problem is compounded for the study of diffusion at low temperatures where it is extremely difficult to conduct the experiments in strict accordance with the conditions imposed by the ideal simple mathematical models.

Conclusions

The development of the anodic-film sectioning technique has permitted the near-surface behavior for low-temperature tracer diffusion in tantalum to come under detailed observation. The shape of the penetration profiles for Nb^{95} in tantalum has been interpreted to be a consequence of the superposition of the contributions of high diffusivity paths to that of pure lattice diffusion. In the temperature range under consideration, an appreciable fraction of the diffusing material is transported along the grain boundaries in polycrystalline specimens. Although contributing very little to the overall mass distribution, the Nb^{95} gradient due to high-diffusivity regions in single crystals was easily observed.

The values obtained for the diffusion coefficients for bulk (lattice) diffusion of Nb^{95} in tantalum agree well with that predicted by a consideration of the extrapolated high-temperature data of Eager

and Langmuir, but not with the low-temperature data of other investigators. It is felt that this discrepancy may be a result of the large effect on the penetration profile of even a very low density of short-circuit paths. For example, the present results point out that even for single crystals, in some cases it is necessary to focus attention upon the first thousand angstroms or so of penetration in order to minimize effects of this type. It is thus apparent that low-temperature diffusion profiles, for this system and probably generally, must be examined carefully in order for the resulting diffusion coefficients to be meaningful.

Acknowledgments

The authors are especially grateful to J. V. Cathcart and F. R. Winslow for many helpful suggestions as well as their assistance with the manuscript. We also wish to thank R. A. Padgett and J. J. Campbell for their contributions to the experimental work.

References

1. V. D. Ignatkov and V. E. Kosenko, Fiz. Tverd. Tela 4, 1627 (1962) [Soviet Phys.-Solid State 4, 1193 (1962)].
2. G. P. Williams, Jr., and L. Slifkin, Acta Met. 11, 319 (1963), and Phys. Rev. Letters 7, 243 (1958).
3. D. L. Styrus and C. T. Tomizuka, J. Appl. Phys. 34, 1001 (1962).
4. R. E. Pawel and T. S. Lundy, J. Appl. Phys. 35, 435 (1964).
5. T. S. Lundy and J. F. Murdock, J. Appl. Phys. 33, 1671 (1962).
6. B. I. Boltaks and V. I. Sokolov, Fiz. Tverd. Tela 6, 771 (1964).
7. R. W. Redington, Phys. Rev. 87, 1066 (1952).
8. R. E. Pawel, Accepted for publication in Rev. Sci. Instr. (1964).
9. P. L. Gruzin and V. I. Meshkov, Vestn. Akad. Nauk Kaz. SSR 11, 85 (1955) [Trans: AEC-TR-2926].
10. N. L. Peterson, Diffusion in Refractory Metals, WADD-TR-60-793 (Mar., 1961), p. 33, and references therein.
11. E. W. Hart, Acta Met. 5, 597 (1957).
12. D. Turnbull and R. E. Hoffman, Acta Met. 2, 419 (1954).
13. G. R. Love, Acta Met. 12, 731 (1964); and P. G. Shewmon and G. R. Love, Acta Met. 11, 899 (1963).

14. G. A. Shirn, E. S. Wajda, and H. B. Huntington, Acta Met. 1, 513 (1953).
15. A. F. Brown and D. A. Blackburn, Acta Met. 11, 1017 (1963).
16. A. J. Mortlock, Acta Met. 12, 675 (1964).
17. D. S. Tannhauser, J. Appl. Phys. 27, 622 (1956).
18. T. S. Lundy and R. E. Pawel, to be published.
19. R. E. Pawel, J. V. Cathcart, and J. J. Campbell, Acta Met. 10, 149 (1962).
20. R. L. Eager and D. B. Langmuir, Phys. Rev. 89, 911 (1953).

4. ZIRCONIUM METALLURGY

M. L. Picklesimer

We are conducting research along several lines on zirconium-base alloys of potential use as structural materials for water cooled and/or moderated reactor systems. The principal projects presently under way are: (1) studies of the physical metallurgy, consisting of transformation kinetics and morphologies, mechanical properties, phase diagrams, and heat-treatment response; (2) the development, evaluation, and utilization of preferred orientation and strain anisotropy in α -zirconium alloys during fabrication, and the utilization of the yield stress anisotropy in increasing the maximum permissible design stresses in structures; (3) the determination of the effects of composition, temperature, and environment on the oxidation-corrosion rates in the thin film stages of oxide growth; (4) a study of the effects of alloy composition and oxidation environment on the structural properties of thin oxide films in situ; and (5) investigation of stress reorientation of hydrides in Zircaloy-2.

Zirconium Alloys

W. G. Northcutt¹ M. L. Picklesimer

Physical metallurgy studies of zirconium alloys this quarter were confined to a determination of the electrical resistivity of a series of zirconium-titanium alloys as a function of temperature at heating and cooling rates ranging from 2 to 8°C/min. We performed the study as a preliminary to one Mr. Northcutt will make during the coming year at the University of Tennessee to determine the specific heat of the same materials.

We used materials of nominally 0, 25, 40, 50, 60, 75, and 100 at. % iodide titanium, remainder iodide zirconium. Drop-cast ingots, 1/2 in. in diameter and 4 in. long, were annealed for 2 hr in high-purity argon at 50 to 75°C above the $\beta/\alpha + \beta$ temperature and swaged to 0.130 in. in

¹Summer employee, presently Graduate Student, Department of Chemical and Metallurgical Engineering, University of Tennessee.

diameter. Intermediate anneals were conducted in evacuated quartz capsules lined with zirconium foil after each 40% reduction in the cross-sectional area.

The collection of the electrical resistivity data is not complete. The data that we have examined show that the Zr-25% at. % Ti alloy had an anomalously higher electrical resistivity than would be expected from the resistivities of the other alloys. No ordering or aging behavior was detected in the Zr-50 at. % Ti alloy, although such reactions have been previously reported in the literature. This does not mean that such behavior does not occur, only that it does not affect the electrical resistivity if it does occur.

Cold-worked specimens were held for 2 hr in argon in a temperature gradient from about 450 to 900°C and water quenched. At least four thermocouples were mounted along the length of each specimen. Longitudinal sections were metallographically prepared but have not been completely examined microscopically. We shall obtain data for the (1) recrystallization temperature, (2) grain growth temperatures in both α and β phases, (3) secondary recrystallization temperatures, if such occur below 900°C, and (4) the temperature limits of the $\alpha + \beta$ fields for these specific materials.

Anisotropy in Zircaloy-2

P. L. Rittenhouse

M. L. Picklesimer

An apparatus for determining the stress-strain anisotropy in biaxial stressing of Zircaloy-2 tubing as a function of preferred orientation has been under design and construction for several months. The quantities that can be measured are (1) axial stress and strain under tension or compression, (2) torsional stress and strain, (3) changes of internal volume, and (4) the uniformity of local strain behavior. The specimens will be tested at varied internal pressures, which will be held constant for each test. Either stress or strain in the axial and torsional directions will be programmed, and axial stress and strain, torsional stress and strain, and internal volume will be continuously recorded. The uniformity of local strain behavior will be determined by photographically recording the distortions of a grid of 1/16-in. squares

placed on the gage section by anodizing. At least 10 photographs will be made during each test. The apparatus will handle tubing from 1/2 to 1-in. OD with 0.030 to 0.06-in. walls.

The frame of the testing apparatus has been assembled, most of the parts for the test heads have been machined and some have been heat treated, the hydraulic ram for axial loading has been obtained, and all of the necessary instrumentation is on hand. The testing equipment should be completed and preliminary testing should be under way by the end of the coming quarter.

The Effect of Preferred Orientation and Stress on the
Directional Precipitation of Hydrides in Zircaloy-2

P. L. Rittenhouse

Our research this quarter has been conducted with the principal aim of the examination of the earlier conclusion² that appreciable redistribution of hydrides precipitated under elastic stress occurs only when that stress is parallel to a density of basal poles (crystallographic texture) considerably greater than random. In this series of tests the hydrogen content was considered as another variable. Schedule J Zircaloy-2³ was selected as the test material because it has a high concentration of basal poles in the transverse direction.⁴

All specimens were vacuum annealed at 800°C, cooled to 650 to 700°C, hydrided to nominal levels of 50, 150, and 250 ppm H₂, homogenized for 1 hr, and slow cooled to room temperature. They were then reheated to 400°C in air, loaded (20,000 psi max), and the hydrides allowed to precipitate

²P. L. Rittenhouse, Fuels and Materials Development Program Quart. Progr. Rept. June 30, 1964, ORNL-TM-920, p. 60.

³P. L. Rittenhouse and M. L. Picklesimer, Metallurgy of Zircaloy-2 Part I. The Effects of Fabrication Variables on the Anisotropy of Mechanical Properties, ORNL-2944, p. 15 (Oct. 13, 1960).

⁴P. L. Rittenhouse and M. L. Picklesimer, Metallurgy of Zircaloy-2 Part II. The Effects of Fabrication Variables on the Preferred Orientation and Anisotropy of Strain Behavior, ORNL-2948, p. 18 (Jan. 11, 1961).

under stress during furnace cooling. These specimens, plus the controls, were sectioned to give three orthogonal planes of examination. The angles between the hydride traces and a reference direction,⁵ the hydride density (particles per square centimeter), and the volume fraction of hydrides were determined on each plane of examination.

Smoothed histograms of the percent of hydride traces in each 5° increment from the reference direction were then obtained. These were combined with the hydride density values to give plots of the number of hydride traces per square centimeter in each 5° increment. Typical plots are shown in Fig. 4.1.

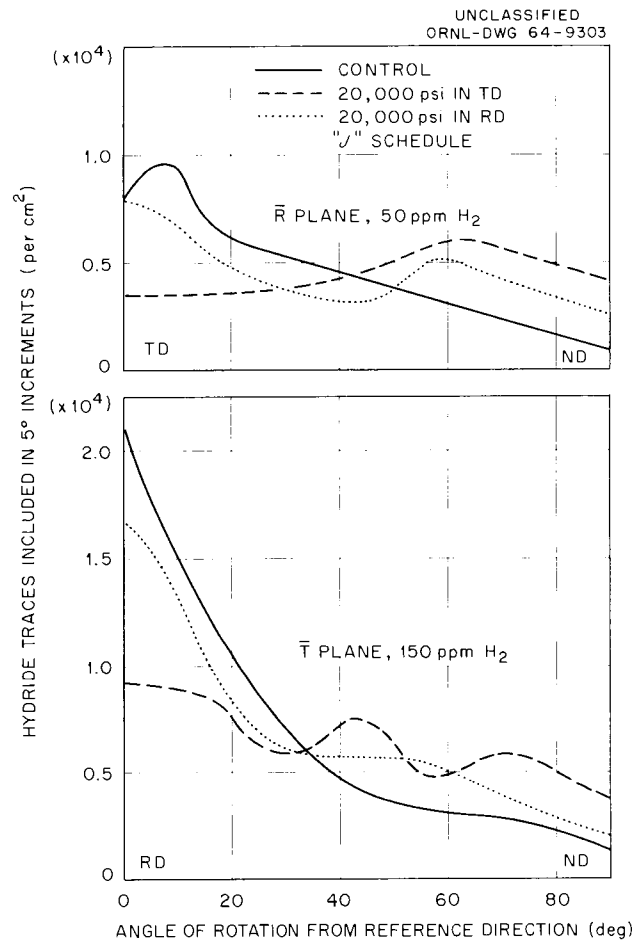


Fig. 1. Portion of the Hydride Trace Data for Schedule J Zircaloy-2.

⁵P. L. Rittenhouse, The Effect of Preferred Orientation and Stress on the Directional Precipitation of Hydrides in Zircaloy-2, ORNL-TM-844 (June 1964).

All data from this series have not been collected or digested. Several tests are still in progress and none of the hydride pole distribution figures⁶ have been determined. This type of figure, previously determined by a trial and error synthesis, will now be obtained through a computer program that has been recently developed for this specific problem. From the data already examined, we can state several conclusions.

1. The data obtained as percent hydride traces in each 5° increment can be misleading. The data must be in terms of the number of hydrides per square centimeter per angular increment. One specific set of data indicated that there had been an appreciable redistribution of hydrides as the hydrogen content was changed for the same stress direction and stress level if only the percent of hydrides in each increment was examined. When the data were converted to the number of hydrides per square centimeter in each increment, it was immediately obvious there were essentially the same number of hydrides per square centimeter for all three hydrogen levels in some increments and that the principal changes were large increases in numbers of hydrides at other positions. This observation indicates that there may well be preferred sites for precipitation that are filled up at low hydrogen levels, and that higher hydrogen levels force less favorable sites to then be occupied.

2. The original conclusion on the relationship between stress direction and density of basal poles seems to be confirmed. The elastic stress in the transverse direction (parallel to a concentration of basal poles) caused considerably more redistribution of hydrides than did stress in the rolling direction.

3. The number of hydrides at any angle in the control specimens (unstressed) is a function of hydrogen content, the percent of the total at each angle being identical for all three levels of hydrogen.

⁶M. L. Picklesimer and P. L. Rittenhouse, Fuels and Materials Development Program Quart. Progr. Rept. June 30, 1964, ORNL-TM-920, pp. 60, 66-68.

4. The higher the hydrogen content, the greater is the number of hydrides reoriented but the fraction reoriented is less.

5. The average hydride particle size is essentially independent of the hydrogen level under the conditions of testing.

6. The redistribution of hydrides increases as the stress increases.

After the present series of test is completed, we shall begin the study of the hydride behavior in single crystals and very large grained Zircaloy-2. We hope to determine the crystallographic habit plane for the hydride, to test the effect of stress in unique crystallographic directions, and to determine the effects of grain boundaries and grain boundary restraints.

Optical Properties of Zirconium Alloys

L. T. Larson⁷

M. L. Picklesimer

The anisotropy of α -zirconium and its alloys in polarized light microscopy is a potential tool for determining information on many properties and aiding in understanding the alloying behavior of many elements. Quantitative measurements of such optical properties as ellipticity, rotation angle, Berek angle, absolute reflectivities, uniaxial reflectivities, indices of refraction, and absorption coefficients, all as functions of wavelength and crystallographic section, should yield information on the electron band structure as affected by alloying elements, provide necessary data of the base-metal properties for the optical study of oxide films in situ, provide the data to permit a unique determination of the crystallographic orientation of an individual grain in space from a single surface examination, and provide the background information necessary for the determination of preferred orientation by polarized light microscopy. These data will be used to study such things as the variation of microtexture from the surface to the center of the wall of tubing as a function of fabrication procedures and alloy content; why hydrides precipitate in some grain

⁷Consultant, Department of Geology, University of Tennessee.

boundaries and not in others that appear equally favorable; the effects of restraint on the deformation systems operating in single-, bi-, and multicrystal specimens of the alloys; solubility limits in the α phase; the growth of single- and bicrystal specimens of α alloys; and the effects of alloying elements on the oxidation-corrosion mechanisms in α alloys.

There have been few previous attempts to make the necessary measurements on any metal, practically all of the prior measurements have been made on opaque minerals, and there is little theory of optical properties of metals (or of solids) that appears to be pertinent. We have obtained and modified a Reichert Zetapan Pol microscope to make measurements that we believe are necessary. Accessory equipment has been purchased or designed and built as we have become aware of the need. The principal remaining equipment problem appears to be the obtention of either an ultrastable high-intensity light source of the proper spectral properties or a compensating double-beam photometer system that will produce readings unaffected by moderate fluctuations of the incident light.

We have measured the ellipticity and angle of rotation as functions of wavelength of the incident light for a number of flat single crystals of zirconium of known crystallographic orientation. Zirconium was found to be "optically positive" at wavelengths from 655 to about 490 $m\mu$, "optically negative" from about 490 to 400 $m\mu$, and again "optically positive" at wavelengths less than about 400 $m\mu$. In optical practice, the following definitions are arbitrarily given: "optically positive" is the rotation of the reflected polarized light toward the principal optical axis (basal pole in zirconium) and "optically negative" is the rotation away from the optical axis. For optically positive material, the index of refraction for the extraordinary ray is greater than that for the ordinary ray; for optically negative material, the index of refraction for the ordinary ray is greater. The angle of rotation of the polarized light incident at the 45° position of a prism plane decreases from about $+2.8^\circ$ at 655 $m\mu$ to 0 at 480 $m\mu$ to -0.4° at 448 $m\mu$, increases to 0 at 395 $m\mu$ and to about $+0.3^\circ$ at 380 $m\mu$. The ellipticity remains positive at all wavelengths but follows approximately the shape of the curve for the angle of rotation. Both the angle of rotation and

the ellipticity decrease in absolute value as the crystallographic section approaches that of the basal plane, where both are zero at all wavelengths because the basal plane is an "isotropic surface."

It appears feasible to use measurements of the angle of rotation and the ellipticity, combined with the sensitive tint method for determining the basal plane trace, to uniquely determine the orientation in space of the crystal lattice of a single grain from a single surface examination. The measurements obtained to date are not sufficiently precise but do show the promise of the technique.

We also measured the angle of rotation, the Berek angle, and the ellipticity vs wavelength on some of the same specimens after anodizing at voltages from 10 to 100 v. These measurements vary appreciably with oxide film thickness and the variation is not understood. The variations observed indicate that it should be possible to find some combination of oxide film thickness, wavelength, and optical property measurement that will be optimum for ease and accuracy of the measurement of grain orientation.

The data indicate that the optical properties of zirconium do not vary monotonically with crystallographic angle from the basal plane at any given wavelength. Presently available optical theory for transparent insulating solids requires that the variation be monotonic and sinusoidal. Since the data collected have been obtained from some eight flat specimens, which have been reprepared several times each during the course of the measurements, the variations observed may have resulted from variations in specimen preparation (the reproducibility after reparation was amazingly good), tilting of the plane of examination from that originally determined by x-ray diffraction, or difficulties encountered in accurately aligning and orienting several of the smaller specimens. We have designed and constructed a five-axis goniometer stage that will allow examination of single-crystal spheres from $1/4$ to $1/2$ in. in diameter. The spheres can be accurately aligned under the microscope and the optical properties determined for any selected crystallographic plane without the necessity of preparing a multitude of flat specimens. The sphere is mounted on an x-ray goniometer head so that the specimen can be transferred to x-ray diffraction equipment for accurate orientation by x-ray diffraction patterns.

Preparation of Single Crystals of Zirconium and Zirconium Alloys

J. C. Wilson

The yield of α -zirconium single crystals produced by zone melting of 3/8-in.-diam cylindrical bars⁸ has been at least doubled (to about 60%) by seeding. A single crystal or large-grained specimen produced in a previous run is used as a seed and is welded to the bar to be zoned at the start of the melting pass. Some improvement in yield was also effected earlier by using a radiation shield part way around the bar in the region behind the molten zone. The shield was introduced to cause the α - β interface to tilt away from the plane normal to the bar axis. Thus, boundaries between neighboring grains could be induced to grow out of the bar and produce a single grain in the cross section in a shorter traverse.

We constructed an electrical discharge machining apparatus to cut sections of single crystals of zirconium. The zirconium crystals that we have obtained are so soft (less than 50 VHN) that they are deformed by the restraining forces necessary to hold them for sawing or abrasive cutting. The apparatus will be used to shape specimens for oxidation and corrosion testing, studies of deformation systems, determinations of mechanical properties, and studies of optical properties. Simple cut-off operations in a 1/2-in.-diam bar require about 40 min. The cut surface is sufficiently flat to be smoothed by chemical polishing.

We used electrical discharge machining to produce a 5/8-in.-diam sphere (about 80% a single crystal) for a preliminary study of the optical properties. The zoned bar was rotated about the bar axis and a slotted piece of brass tubing was used as the cutting tool. The machining time for roughing the sphere was about 8 hr, and final machining required about the same time. The cut surface was sufficiently smooth to be finished by chemical polishing, and the disturbed layer at the surface (evidenced by fine twins) was removed before chemical

⁸J. C. Wilson, Fuels and Materials Development Program Quart. Progr. Rept. June 30, 1964, ORNL-TM-920, pp. 70-74.

polishing had completely smoothed the surface. The equipment is being modified to incorporate a rotating cutting tube since this will automatically produce a more spherical specimen.

A stereomicroscope was fitted with a polarized light attachment to examine crystals under polarized light and sensitive tint conditions. The contrast between neighboring grains of different orientations is much sharper and appears in brilliant colors. This addition also makes possible the approximate determination of the basal plane traces and basal pole orientation in large bar and strip specimens. The macro-examination of zoned stock has been considerably eased and improved.

Zone Refining of Zirconium

J. C. Wilson

The feasibility of zone refining bars of zirconium up to at least 3/4-in. in diameter was demonstrated by zone melting an as-deposited crystal bar that measured 3/4 in. across the flats. This was the maximum size specimen that could be passed through the gun of the equipment presently in use.

The contamination of zirconium during zone refining in the present apparatus (pressure during zoning is in the low 10^{-8} torr range) appears to limit the minimum oxygen concentration attainable to about 40 ppm after 9 passes at 2 in/hr. The oxygen concentration was fairly uniform along a 9- or 10-pass bar, but not in bars with only 4 passes. Thus, it appears that the oxygen level was finally determined by the offsetting effects of zoning and recontamination from the system. Carbon contamination appears to be of the order of a few parts per million per pass, and the carbon has tended to go to the tail of the bar.

We expect that larger starting materials can be used and higher purifications obtained in the ultrahigh vacuum apparatus presently being constructed for zoning.

Properties of High-Purity Zirconium

J. C. Wilson

Now that many of the problems of purification and single-crystal growth in zirconium have been solved, we can begin the study of the properties of the purified metal and of the effects of trace impurities and alloying elements on those properties.

Of special interest are the effects of impurities on the oxidation and water-corrosion of purified zirconium. Zone-refined bars were cold rolled to 0.04-in.-thick strip for corrosion testing, and annealing studies are now under way to determine the optimum heat treatment for placing the corrosion specimens in the same metallurgical condition. Recrystallization and grain growth studies were conducted at temperatures from 250 to 900°C. Specimens were taken from the head, center, and tail portions of the zone-refined bar. This, in effect, provides three levels of several impurities. We found that specimens taken from the head end of the bar completely recrystallized in less than 2 hr at 250°C. The specimens from the three regions of the zoned bar are distinguishably different from each other and from the unrefined starting stock at all annealing temperatures, indicating that the zone purification has caused appreciable effects on the behavior of the material. The examination of these specimens is continuing.

Oxide Film Studies

J. C. Banter

A new method for the determination of the refractive indices and thicknesses of thin oxide films formed anodically on zirconium was recently reported.⁹ Transmission interference measurements are made on oxide films stripped from the metal. These measurements have since been made on anodic films whose thicknesses varied from approximately 3000 to 5500 Å. The results indicate that, within experimental error, the refractive indices of these films were independent of the film

⁹J. C. Banter, Fuels and Materials Development Program Quart. Progr. Rept. June 30, 1964, ORNL-TM-920, pp. 68-70.

thickness over this thickness range. We also noted that the refractive index measured by this technique was not necessarily the same as that of the oxide film in situ. The removal of the metal from the films should relieve much of the strain that had existed in the film. This relief should affect the optical properties but should not significantly change the physical thickness. Thicknesses measured by the transmission interference technique were used in conjunction with reflection interference measurements to calculate the refractive indices of the films in situ.

The interference maxima produced in the light reflected from the anodized zirconium specimens are described by the equation

$$T \sqrt{n^2 - \sin^2 i} - \frac{\delta'' \lambda}{4\pi} = \frac{m\lambda}{2} \quad , \quad (1)$$

where n is the refractive index of the oxide film, T is its thickness, i is the angle of incidence of the light, λ is the wavelength at which the maximum occurs, m is the order of interference, and δ'' is the phase change that occurs upon reflection from the oxide-metal interface. The wavelengths at which the maxima occurred were measured with a spectrophotometer for two specimens with films of different thicknesses, T_1 and T_2 , and the quantity $m\lambda/2$ was plotted against wavelength for each specimen. The difference, D , between the two curves obtained at any given wavelength is then

$$D = (T_2 - T_1) \sqrt{n^2 - \sin^2 i} \quad . \quad (2)$$

By determining T_2 and T_1 by the transmission interference measurements, n may then be calculated for the films in situ if it is assumed that their refractive indices are independent of film thickness as are those of the stripped oxide films.

The refractive indices of stripped and in situ films are compared in Fig. 4.2. These curves indicate that the refractive indices of the stripped film are lower than those of the films in place on the metal. It is generally observed that the refractive indices increase with an

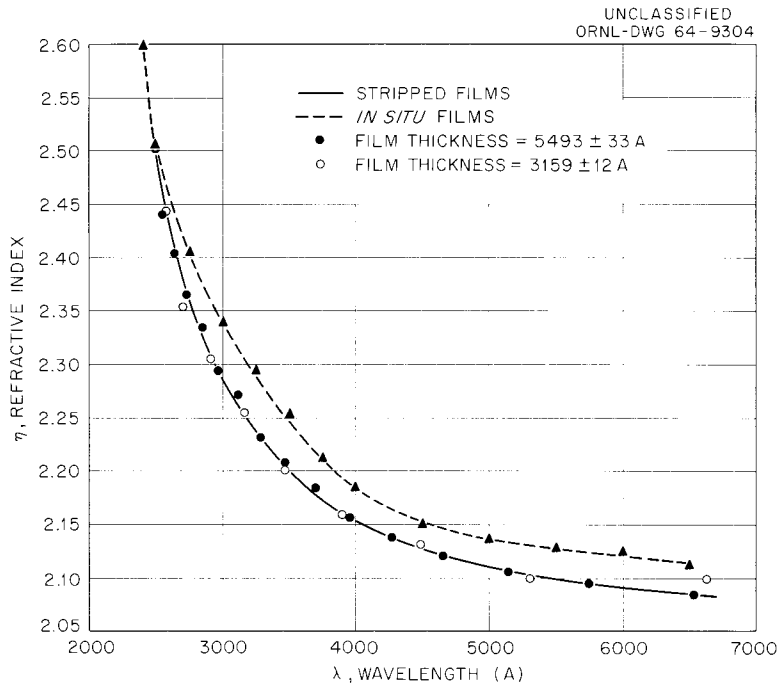
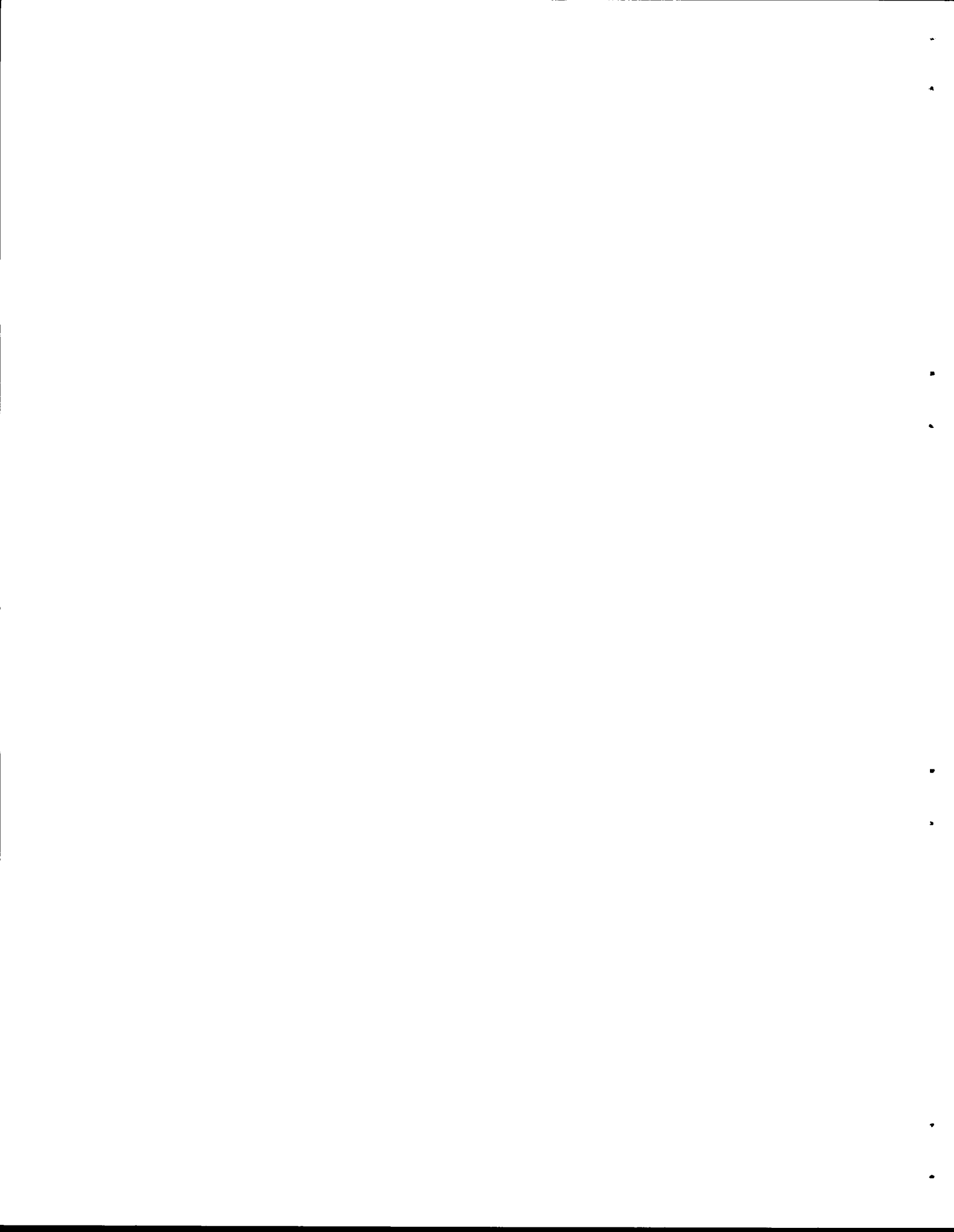


Fig. 4.2. Comparison of Refractive Indices for Anodized Films In Situ and Stripped from Zirconium Foil.

increase in density of the material, and the lower indices of refraction for the stripped films is in agreement with the concept of the relief of strain in the films by the removal of the metal. We have not been able to determine the magnitude of the strain present in the film in situ but an experimental evaluation is planned in the near future. The technique will involve measuring the deflection of a foil specimen during anodization of one surface only.

The first report in this series is:

ORNL-TM-920 Period Ending June 30, 1964



INTERNAL DISTRIBUTION

1-3.	Central Research Library	63.	T. S. Lundy
4-5.	ORNL - Y-12 Technical Library	64.	R. N. Lyon
	Document Reference Section	65.	H. G. MacPherson
6-15.	Laboratory Records	66.	R. E. MacPherson
16.	Laboratory Records, RC	67.	M. M. Martin
17.	ORNL Patent Office	68.	W. R. Martin
18.	G. M. Adamson, Jr.	69.	R. W. McClung
19.	J. C. Banter	70.	H. E. McCoy, Jr.
20.	J. H. Barrett	71.	H. C. McCurdy
21.	S. E. Beall	72.	R. E. McDonald
22.	M. Bender	73.	D. L. McElroy
23.	R. G. Berggren	74.	C. J. McHargue
24.	J. O. Betterton, Jr.	75.	M. C. McIlwain
25.	D. S. Billington	76.	F. R. McQuilkin
26.	A. L. Boch	77.	A. J. Miller
27.	B. S. Borie	78.	E. C. Miller
28.	W. H. Bridges	79.	F. H. Neill
29.	R. B. Briggs	80.	S. M. Ohr
30.	W. E. Brundage	81.	P. Patriarca
31.	J. V. Cathcart	82.	A. M. Perry
32.	G. W. Clark	83.	M. L. Picklesimer
33.	K. V. Cook	84.	P. L. Rittenhouse
34.	J. H. Crawford	85.	M. W. Rosenthal
35.	J. E. Cunningham	86.	G. Samuels
36.	J. H. DeVan	87.	H. W. Savage
37.	C. V. Dodd	88.	W. Schüle
38.	D. A. Douglas, Jr.	89.	J. L. Scott
39.	J. I. Federer	90.	O. Sisman
40.	B. E. Foster	91.	G. M. Slaughter
41.	A. P. Fraas	92.	G. P. Smith, Jr.
42.	J. H. Frye, Jr.	93.	S. D. Snyder
43.	R. J. Gray	94.	I. Spiewak
44.	B. L. Greenstreet	95.	J. T. Stanley
45.	W. R. Grimes	96.	W. J. Stelzman
46.	J. P. Hammond	97.	J. O. Stiegler
47.	W. O. Harms	98.	J. A. Swartout
48.	R. L. Heestand	99.	A. Taboada
49-53.	M. R. Hill	100.	W. C. Thurber
54.	N. E. Hinkle	101.	D. B. Trauger
55.	H. W. Hoffman	102.	G. M. Watson
56.	H. Inouye	103.	M. S. Wechsler
57.	T. N. Jones	104.	A. M. Weinberg
58.	G. W. Keilholtz	105.	J. R. Weir
59.	B. C. Kelley	106.	W. J. Werner
60.	J. A. Lane	107.	G. D. Whitman
61.	C. F. Leitten, Jr.	108.	J. M. Williams
62.	A. L. Lotts	109.	R. O. Williams

- | | |
|-----------------------|-----------------------|
| 110. J. C. Wilson | 113. F. W. Young, Jr. |
| 111. F. R. Winslow | 114. C. S. Yust |
| 112. H. L. Yakel, Jr. | 115. J. C. Zukas |

EXTERNAL DISTRIBUTION

- 116. A. J. Alexander, AEC, CANEL
- 117. R. J. Allio, Westinghouse Atomic Power Division
- 118. R. D. Baker, Los Alamos Scientific Laboratory
- 119. L. Brewer, University of California, Berkeley
- 120. V. P. Calkins, GE, NMPO
- 121. W. Cashin, Knolls Atomic Power Laboratory
- 122. R. M. Cilimberg, Division of Reactor Development,
AEC, Washington
- 123-124. D. F. Cope, AEC, ORO
- 125. G. K. Dicker, Division of Reactor Development,
AEC, Washington
- 126. E. A. Evans, GE, Hanford
- 127. W. C. Francis, Phillips Petroleum Company
- 128. R. G. Grove, Mound Laboratory
- 129. D. H. Gurinsky, BNL
- 130. S. Hasko, NBS
- 131. A. N. Holden, GE, APED
- 132. J. S. Kane, University of California, Livermore
- 133. J. H. Kittel, ANL
- 134. E. J. Kreih, Westinghouse, Bettis Atomic Power
Laboratory
- 135. W. L. Larsen, Iowa State University, Ames Laboratory
- 136. J. H. MacMillan, Babcock and Wilcox Company
- 137. R. E. Pahler, Division of Reactor Development,
AEC, Washington
- 138. S. Paprocki, BMI
- 139. D. Ragone, GA
- 140. L. M. Raring, Pratt & Whitney, CANEL
- 141. Research and Development, AEC, ORO
- 142. A. H. Roberson, U. S. Department of the Interior,
Bureau of Mines
- 143. W. Rostokev, Illinois Institute of Technology
Research Institute
- 144. F. C. Schwenk, Division of Reactor Development,
AEC, Washington
- 145-146. J. M. Simmons, Division of Reactor Development,
AEC, Washington
- 147. L. E. Steele, Naval Research Laboratory
- 148. R. H. Steele, Division of Reactor Development,
AEC, Washington
- 149. W. F. Sheely, Division of Research,
AEC, Washington
- 150. A. Strasser, United Nuclear Corporation

151. W. R. Voigt, Division of Reactor Development,
AEC, Washington
152. C. E. Weber, Atomics International
153. G. W. Wensch, Division of Reactor Development,
AEC, Washington
154. M. J. Whitman, Division of Reactor Development,
AEC, Washington
- 155-169. Division of Technical Information Extension